

MIT Open Access Articles

Measurements of production cross sections of polarized same-sign W boson pairs in association with two jets in proton-proton collisions at $\sqrt{s}=13$ TeV

The MIT Faculty has made this article openly available. **Please share** how this access benefits you. Your story matters.

Citation: Harris, Philip. 2021. "Measurements of production cross sections of polarized same-sign W boson pairs in association with two jets in proton-proton collisions at $\sqrt{s}=13$ TeV." Physics Letters, Section B: Nuclear, Elementary Particle and High-Energy Physics, 812.

As Published: 10.1016/J.PHYSLETB.2020.136018

Publisher: Elsevier BV

Persistent URL: <https://hdl.handle.net/1721.1/142088>

Version: Final published version: final published article, as it appeared in a journal, conference proceedings, or other formally published context

Terms of use: Creative Commons Attribution 4.0 International license





Measurements of production cross sections of polarized same-sign W boson pairs in association with two jets in proton-proton collisions at $\sqrt{s} = 13$ TeV

The CMS Collaboration ^{*}

CERN, Geneva, Switzerland

ARTICLE INFO

Article history:

Received 20 September 2020
 Received in revised form 18 November 2020
 Accepted 8 December 2020
 Available online 11 December 2020
 Editor: M. Doser

Keywords:

CMS
 Diboson
 Electroweak
 Polarized
 Longitudinal

ABSTRACT

The first measurements of production cross sections of polarized same-sign $W^{\pm}W^{\pm}$ boson pairs in proton-proton collisions are reported. The measurements are based on a data sample collected with the CMS detector at the LHC at a center-of-mass energy of 13 TeV, corresponding to an integrated luminosity of 137 fb^{-1} . Events are selected by requiring exactly two same-sign leptons, electrons or muons, moderate missing transverse momentum, and two jets with a large rapidity separation and a large dijet mass to enhance the contribution of same-sign $W^{\pm}W^{\pm}$ scattering events. An observed (expected) 95% confidence level upper limit of 1.17 (0.88) fb is set on the production cross section for longitudinally polarized same-sign $W^{\pm}W^{\pm}$ boson pairs. The electroweak production of same-sign $W^{\pm}W^{\pm}$ boson pairs with at least one of the W bosons longitudinally polarized is measured with an observed (expected) significance of 2.3 (3.1) standard deviations.

© 2020 The Author(s). Published by Elsevier B.V. This is an open access article under the CC BY license (<http://creativecommons.org/licenses/by/4.0/>). Funded by SCOAP³.

1. Introduction

Vector boson scattering (VBS) processes probe the electroweak (EW) symmetry breaking mechanism at high energy scales. The unitarity of the tree-level amplitude of the scattering of longitudinally polarized gauge bosons at high energies is restored in the standard model (SM) by a Higgs boson with a mass lower than about 1 TeV [1,2]. The observation of a Higgs boson with a mass of about 125 GeV [3–5] provides an explanation that W and Z gauge bosons acquire mass via the Brout–Englert–Higgs mechanism, but additional Higgs bosons may still play a role in the EW symmetry breaking. Modifications of the VBS cross section for the longitudinally polarized W and Z bosons are predicted in models of physics beyond the SM through modifications of the Higgs boson couplings to gauge bosons or through the presence of new resonances [6,7]. The measurements of the longitudinally polarized scattering of the W and Z bosons provide complementary information to direct measurements of the Higgs boson couplings to gauge bosons [8,9]. Models of beyond SM physics that modify the cross sections of VBS processes with transversely polarized W and Z bosons are discussed in Ref. [10].

At the CERN LHC, VBS interactions are characterized by the presence of two gauge bosons in association with two forward jets

that have a large rapidity separation. They are part of a class of processes contributing to the same-sign $W^{\pm}W^{\pm}$ production in association with two jets that proceeds via the EW interaction at tree level, $\mathcal{O}(\alpha^4)$, where α is the EW coupling, referred to as EW $W^{\pm}W^{\pm}$ production. The leptonic decay mode $W^{\pm}W^{\pm} \rightarrow \ell^{\pm}\nu\ell'^{\pm}\nu$, where both W bosons decay into electrons or muons, $\ell, \ell' = e, \mu$, is a promising final state to study the polarized scattering from gauge bosons. The background contribution of the quantum chromodynamics (QCD) induced production of $W^{\pm}W^{\pm}$ boson pairs in association with two jets with tree-level contributions at $\mathcal{O}(\alpha^2\alpha_s^2)$, where α_s is the strong coupling, is small. Fig. 1 shows representative Feynman diagrams of VBS processes involving self-interactions between gauge bosons through triple and quartic gauge couplings and the t-channel Higgs boson exchange.

The unpolarized EW $W^{\pm}W^{\pm}$ production has been previously measured at the LHC in the leptonic decay modes at $\sqrt{s} = 8$ and 13 TeV [11–15]. The first differential cross section measurements were reported in Ref. [15]. This Letter presents the first measurement of the EW production cross sections for polarized same-sign $W^{\pm}W^{\pm}$ boson pairs. The data sample of proton-proton (pp) collisions at $\sqrt{s} = 13$ TeV corresponds to an integrated luminosity of 137 fb^{-1} [16–18], collected with the CMS detector [19] in three LHC operating periods during the years 2016, 2017, and 2018. The three data sets are analyzed independently, with appropriate calibrations and corrections, because of the various LHC operating conditions and the upgrades in the performance of the CMS de-

^{*} E-mail address: cms-publication-committee-chair@cern.ch.

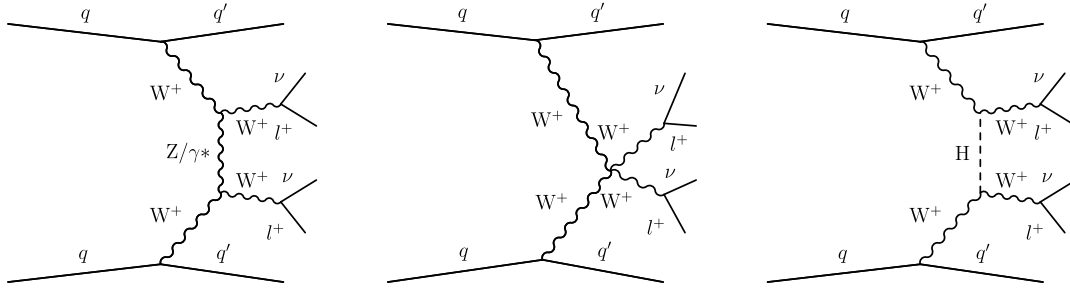


Fig. 1. Illustrative Feynman diagrams of VBS processes, where W bosons are radiated from incoming quarks (q), contributing to the EW-induced production of events containing two forward jets and $W^\pm W^\pm$ boson pairs decaying to leptons. Diagrams with the triple gauge coupling vertex (left), the quartic gauge coupling vertex (center), and the t -channel Higgs boson exchange (right) are shown.

detector. Candidate events contain exactly two identified same-sign leptons, moderate missing transverse momentum, and two jets with a large rapidity separation and a high dijet mass.

In the $W^\pm W^\pm$ channel, each of the W bosons can be polarized either longitudinally (W_L) or transversely (W_T), leading to three distinct contributions $W_L^\pm W_L^\pm$, $W_L^\pm W_T^\pm$, and $W_T^\pm W_T^\pm$. Ideally, we would measure all three contributions separately, but the current data sample size is too limited. Therefore, two maximum-likelihood fits are performed: one for $W_L^\pm W_L^\pm$ and $W_X^\pm W_T^\pm$; and another for $W_L^\pm W_X^\pm$ and $W_T^\pm W_T^\pm$. The index X indicates either of the two polarization states. The event kinematical properties are used to extract the various contributions. Two sets of results are reported with the helicity eigenstates defined either in the WW center-of-mass reference frame or in the initial-state parton-parton one.

2. The CMS detector

The central feature of the CMS apparatus is a superconducting solenoid of 6 m internal diameter, providing a magnetic field of 3.8 T. Within the solenoid volume are a silicon pixel and strip tracker, a lead tungstate crystal electromagnetic calorimeter (ECAL), and a brass and scintillator hadron calorimeter, each composed of a barrel and two endcap sections. Forward calorimeters extend the pseudorapidity (η) coverage provided by the barrel and endcap detectors. Muons are detected in gas-ionization detectors embedded in the steel flux-return yoke outside the solenoid. A more detailed description of the CMS detector, together with a definition of the coordinate system used and the relevant kinematic variables, is given in Ref. [19].

The first level of the CMS trigger system, composed of custom hardware processors, uses information from the calorimeters and muon detectors to select events of interest with a latency of less than 4 μ s. The second level, known as the high-level trigger, consists of a farm of processors running a version of the full event reconstruction software optimized for fast processing, and reduces the event rate to about 1 kHz before data storage [20].

3. Signal and background simulation

Several Monte Carlo (MC) event generators are used to simulate the signal and background contributions. Three independent sets of simulated events for each process are needed to match the data-taking conditions in the various years. All generated events are processed through a simulation of the CMS detector based on GEANT4 [21] and are reconstructed with the same algorithms used for data. Additional pp interactions in the same and nearby bunch crossings, referred to as pileup, are also simulated. The distribution of the number of pileup interactions in the simulation is adjusted to match the one observed in the data. The average number of pileup interactions was 23 (32) in 2016 (2017 and 2018).

The SM EW $W_L^\pm W_L^\pm$, $W_L^\pm W_T^\pm$, and $W_T^\pm W_T^\pm$ signal processes, where both bosons decay leptonically, are separately simulated using MADGRAPH5_AMC@NLO 2.7.2, with the implementation of polarized parton scattering [22–24], at leading order (LO) with six EW ($\mathcal{O}(\alpha^6)$) and zero QCD vertices. The NNPDF 3.1 next-to-next-to-leading-order (NNLO) [25] parton distribution functions (PDFs) are used. Signal processes are simulated with the helicity eigenstates defined either in the $W^\pm W^\pm$ center-of-mass reference frame or in the initial parton-parton reference frame. The PHANTOM 1.5.1 generator [26,27] uses the on-shell projection technique for the predictions of the signal processes as discussed in Ref. [28]. The MADGRAPH5_AMC@NLO predictions show satisfactory agreement within the statistical uncertainties with the PHANTOM predictions in the relevant fiducial region, defined in Section 8, for this analysis. Comparisons of the MADGRAPH5_AMC@NLO predictions with predictions based on the on-shell projection technique are reported in Ref. [24]. The small contributions of off-shell and nonresonant production [28] are not included in the simulated signal samples and amount to 1–2% in the fiducial region.

The full next-to-leading-order (NLO) QCD and EW corrections for the leptonic unpolarized $W^\pm W^\pm$ scattering process have been computed [29,30], and they reduce the LO cross section for the EW $W^\pm W^\pm$ process by approximately 10–15%, with the correction increasing in magnitude to up to 25% with increasing dilepton and dijet masses. The NLO corrections for the $W_L^\pm W_L^\pm$, $W_L^\pm W_T^\pm$, and $W_T^\pm W_T^\pm$ processes are not known. The corrections for the unpolarized EW $W^\pm W^\pm$ process at orders of $\mathcal{O}(\alpha_s \alpha^6)$ and $\mathcal{O}(\alpha^7)$ are applied to the MADGRAPH5_AMC@NLO LO cross sections for the $W_T^\pm W_T^\pm$ process. Only the corrections at order of $\mathcal{O}(\alpha_s \alpha^6)$ are applied to the MADGRAPH5_AMC@NLO LO cross sections for the $W_L^\pm W_L^\pm$ and $W_L^\pm W_T^\pm$ processes because the corrections at order $\mathcal{O}(\alpha^7)$ are expected to be smaller for the $W_L^\pm W_L^\pm$ and $W_L^\pm W_T^\pm$ processes compared to the size of the corresponding corrections for the unpolarized EW $W^\pm W^\pm$ process [31]. There is a negligible effect in the measured cross sections from differences in the event kinematical properties caused by the treatment of the NLO corrections.

The EW WZ background process is simulated with MADGRAPH5_AMC@NLO 2.4.2 at order $\mathcal{O}(\alpha^6)$. The QCD-induced WZ process is simulated at LO with up to three additional partons in the matrix element calculations using the MADGRAPH5_AMC@NLO generator with at least one QCD vertex at tree level. The different jet multiplicities are merged using the MLM scheme [32] to match matrix element and parton shower jets. The MADGRAPH5_AMC@NLO generator is also used to simulate the QCD-induced $W^\pm W^\pm$ process.

The interference between the EW and QCD diagrams for the $W^\pm W^\pm$ and WZ processes is generated with MADGRAPH5_AMC@NLO including the contributions of order $\alpha_s \alpha^5$. The relative contributions in the fiducial region of the interference term between the EW and the QCD diagrams for the $W_L^\pm W_L^\pm$, $W_L^\pm W_T^\pm$, and

$W_T^\pm W_T^\pm$ processes are comparable to the relative contributions of the $W_L^\pm W_L^\pm$, $W_L^\pm W_T^\pm$, and $W_T^\pm W_T^\pm$ processes to the EW $W^\pm W^\pm$ cross section. The interferences between the signal processes are expected to be small [24], and good agreement is observed between the incoherent sum of the polarized cross sections and the unpolarized cross sections for the distributions of the observables.

The POWHEG v2 [33–37] generator is used to simulate the $t\bar{t}$, tW , and other diboson processes at NLO accuracy in QCD. Production of $t\bar{t}W$, $t\bar{t}Z$, $t\bar{t}\gamma$, and triple vector boson (VVV) events is simulated at NLO accuracy in QCD using the MADGRAPH5_aMC@NLO 2.2.2 (2.4.2) generator for 2016 (2017 and 2018) [22,23] samples. The tZq process is simulated at NLO in the four-flavor scheme using MADGRAPH5_aMC@NLO 2.3.3. The tZq MC simulation is normalized using a cross section computed at NLO with MADGRAPH5_aMC@NLO in the five-flavor scheme, following the procedure described in Ref. [38]. The double parton scattering $W^\pm W^\pm$ production is generated at LO using PYTHIA 8.226 (8.230) [39] for 2016 (2017 and 2018) samples.

The NNPDF 3.0 NLO [40] (NNPDF 3.1 NNLO [25]) PDFs are used for generating all 2016 (2017 and 2018) background samples. For all processes, the parton showering and hadronization are simulated using PYTHIA 8.226 (8.230) for 2016 (2017 and 2018). The modeling of the underlying event is done using the CUETP8M1 [41,42] (CP5 [43]) tune for simulated samples corresponding to the 2016 (2017 and 2018) data.

4. Event reconstruction and selection

Events are reconstructed using the CMS particle-flow (PF) algorithm [44] that reconstructs and identifies each individual particle with an optimized combination of all subdetector information. The missing transverse momentum vector \vec{p}_T^{miss} is defined as the projection onto the plane perpendicular to the beam axis of the negative vector sum of the momenta of all reconstructed PF objects in an event. Its magnitude is referred to as p_T^{miss} .

Jets are reconstructed by clustering PF candidates using the anti- k_T algorithm [45,46] with a distance parameter of 0.4. Jets are calibrated in the simulation, and separately in data, accounting for energy deposits of neutral particles from pileup and any nonlinear detector response [47]. The effect of pileup is mitigated through a charged-hadron subtraction technique, which removes the energy of charged hadrons not originating from the primary vertex (PV) [48] of the event. Corrections to jet energies to account for the detector response are propagated to p_T^{miss} [49]. The PV is defined as the vertex with the largest value of summed physics-object p_T^2 . The physics objects are derived from only the tracks assigned to the vertex as inputs by clustering them into jets, including leptons. The p_T^{miss} is also recalculated only from those jets by summing their negative p_T vectors.

Electrons and muons are reconstructed by associating a track reconstructed in the tracking detectors with either a cluster of energy in the ECAL [50,51] or a track in the muon system [52]. Electron and muon candidates must pass certain identification criteria to be further selected in the analysis. For the “loose” identification, they must satisfy $p_T > 10$ GeV and $|\eta| < 2.5$ (2.4) for electrons (muons). At the final stage of the lepton selection the “tight” working points criteria following the definitions provided in Refs. [50,52] are chosen, including requirements on the impact parameter of the candidates with respect to the PV and their isolation with respect to other particles in the event [9].

For electrons, the background contribution coming from a mismeasurement of the track charge is not negligible. The sign of this charge is evaluated using three observables that measure the electron curvature applying different methods; requiring all three charge evaluations to agree reduces this background contribution

Table 1

Summary of the requirements defining the $W^\pm W^\pm$ SR. The $|m_{\ell\ell} - m_Z|$ requirement is applied to the dielectron final state only.

Variable	Requirement
Leptons	Exactly 2 same-sign leptons, $p_T > 25/20$ GeV
p_T^1	> 50 GeV
$ m_{\ell\ell} - m_Z $	> 15 GeV (ee)
$m_{\ell\ell}$	> 20 GeV
p_T^{miss}	> 30 GeV
b quark veto	Required
$\text{Max}(z_\ell^*)$	< 0.75
m_{jj}	> 500 GeV
$ \Delta\eta_{jj} $	> 2.5

by a factor of five with an efficiency of about 97% [50]. The charge mismeasurement is negligible for muons [53,54].

Collision events are collected using single-electron (single-muon) triggers that require the presence of an isolated lepton with $p_T > 27$ (24) GeV. In addition, a set of dilepton triggers with lower p_T thresholds, with a threshold of 23 GeV or lower for the leading lepton and with a threshold of 8 GeV for the subleading lepton, is used. This ensures a trigger efficiency above 99% for events that satisfy the subsequent offline selection.

Several selection requirements are used to isolate the $W^\pm W^\pm$ topology defining the signal region (SR) while reducing the contributions of background processes. Candidate events contain exactly two isolated same-sign charged leptons and at least two jets with $p_T^1 > 50$ GeV and $|\eta| < 4.7$. Jets that are within $\Delta R = \sqrt{(\Delta\phi)^2 + (\Delta\eta)^2} < 0.4$ of one of the identified leptons are not used in the analysis. Here $\Delta\phi$ and $\Delta\eta$ refer to the differences in the azimuthal angle ϕ and η of the jet and the charged-lepton candidate, respectively. Because of the presence of undetected neutrinos in the signal events, p_T^{miss} is required to exceed 30 GeV.

The $W^\pm W^\pm$ SR selection requires one of the same-sign leptons to satisfy $p_T > 25$ GeV and the other $p_T > 20$ GeV. The mass of the dilepton pair $m_{\ell\ell}$ must be greater than 20 GeV. Candidate events in the dielectron final state within 15 GeV of the nominal Z boson mass m_Z [55] are rejected to reduce the number of Z boson background events where the charge of one of the electron candidates is misidentified.

The VBS topology is targeted by requiring the two highest- p_T jets to have a dijet mass $m_{jj} > 500$ GeV and a pseudorapidity separation $|\Delta\eta_{jj}| > 2.5$. The W bosons in the VBS topologies are mostly produced in the central rapidity region with respect to the two selected jets. The candidate $W^\pm W^\pm$ events are required to satisfy $\text{max}(z_\ell^*) < 0.75$, where $z_\ell^* = |\eta^\ell - (\eta^{j1} + \eta^{j2})/2|/|\Delta\eta_{jj}|$ is the Zeppenfeld variable [56], η^ℓ is the pseudorapidity of one of the selected leptons, and η^{j1} and η^{j2} are the pseudorapidities of the two candidate VBS jets.

Candidate events with one or more jets with $p_T > 20$ GeV and $|\eta| < 2.4$ that are consistent with the fragmentation of a bottom quark are rejected to reduce the number of top quark background events. The DEEPCSV b tagging algorithm [57] is used for this selection. For the chosen working point, the efficiency to select b quark jets is about 70% and the rate for incorrectly tagging jets originating from the hadronization of gluons or u, d, s quarks is about 1%. The rate for incorrectly tagging jets originating from the hadronization of c quarks is about 10%. The selection requirements to define the same-sign $W^\pm W^\pm$ SR are summarized in Table 1.

5. Extracting polarization information

In the $W^\pm W^\pm$ channel, the W bosons can each be either longitudinally or transversely polarized leading to different kinematic distributions, reflected in the kinematical properties of the two leptons, the two jets, and \vec{p}_T^{miss} . The W_L bosons tend to be radiated

Table 2

List and description of all the input variables for the signal BDT trainings.

Variables	Definitions
$\Delta\phi_{jj}$	Difference in azimuthal angle between the leading and subleading jets
p_T^{j1}	p_T of the leading jet
p_T^{j2}	p_T of the subleading jet
$p_T^{\ell_1}$	Leading lepton p_T
$p_T^{\ell_2}$	Subleading lepton p_T
$\Delta\phi_{\ell\ell}$	Difference in azimuthal angle between the two leptons
$m_{\ell\ell}$	Dilepton mass
$p_T^{\ell\ell}$	Dilepton p_T
m_T^{WW}	Transverse WW diboson mass
$z_{\ell_1}^*$	Zeppenfeld variable of the leading lepton
$z_{\ell_2}^*$	Zeppenfeld variable of the subleading lepton
$\Delta R_{j1,\ell\ell}$	ΔR between the leading jet and the dilepton system
$\Delta R_{j2,\ell\ell}$	ΔR between the subleading jet and the dilepton system
$(p_T^{\ell_1} p_T^{\ell_2}) / (p_T^{j1} p_T^{j2})$	Ratio of p_T products between leptons and jets
p_T^{miss}	Missing transverse momentum

at a smaller angle with respect to the incoming quark direction, resulting in a smaller W_L boson p_T compared to the radiated W_T boson p_T . In addition, there are differences in the behavior of the scattering amplitudes as a function of the $W^\pm W^\pm$ center-of-mass energy and the scattering angle [58].

Multivariate techniques are used to enhance the separation between the different processes. We implement boosted decision trees (BDTs) with gradient boosting using the TMVA package [59]. Two different BDTs, referred to as the signal BDTs, are trained on simulated events to separate either the $W_L^\pm W_L^\pm$ and $W_X^\pm W_T^\pm$ processes or the $W_L^\pm W_X^\pm$ and $W_T^\pm W_T^\pm$ processes. Several discriminating observables are used as the inputs to the BDTs, including the jet and lepton kinematical properties and p_T^{miss} , as summarized in Table 2. The distributions of these observables are taken from the SM predictions. Hypothetical modifications due to beyond the SM physics are assumed to impact only the production rates, but not the kinematic distributions of sensitive variables. Angular variables are included, such as the difference in the azimuthal angles between the leading and subleading jets ($\Delta\phi_{jj}$) and leptons ($\Delta\phi_{\ell\ell}$), and the ΔR between the leading (subleading) jet and the dilepton system $\Delta R_{j1,\ell\ell}$ ($\Delta R_{j2,\ell\ell}$). The dilepton $p_T^{\ell\ell}$, $m_{\ell\ell}$, and the transverse diboson mass m_T^{WW} as defined in Ref. [15] are also considered. The kinematic variable $(p_T^{\ell_1} p_T^{\ell_2}) / (p_T^{j1} p_T^{j2})$ proposed in Ref. [58] is also included in the BDT inputs. A larger set of discriminating observables was studied, but only variables that improve the sensitivity and show some separation are retained. The distributions of $\Delta\phi_{jj}$ (upper), $\Delta\phi_{\ell\ell}$ (middle), and $m_{\ell\ell}$ (lower) at the generator level for the $W_L^\pm W_L^\pm$, $W_L^\pm W_T^\pm$, and $W_T^\pm W_T^\pm$ processes with the helicity eigenstates defined in the parton-parton (left) and $W^\pm W^\pm$ (right) center-of-mass reference frames are shown in Fig. 2. The signal extraction was also compared with a deep neural network using the KERAS [60] deep learning library, interfaced with the TENSORFLOW [61] library, which led to a consistently good performance.

6. Background estimation

A combination of methods based on control samples in data and simulation is used to estimate background contributions. Uncertainties related to the theoretical and experimental predictions are described in Section 7. The electron charge misidentification in simulation is corrected to reproduce the rate measured in data. Using $Z \rightarrow ee$ events, the misidentification rate is about 0.01% (0.3%) in the barrel (endcap) region [50]. Oppositely charged dilepton final states from $t\bar{t}$, tW , W^+W^- , and Drell–Yan processes contribute to the background from charge misidentification.

Table 3

List and description of the input variables for the inclusive BDT training.

Variables	Definitions
m_{jj}	Dijet mass
$ \Delta\eta_{jj} $	Difference in pseudorapidity between the leading and subleading jets
$\Delta\phi_{jj}$	Difference in azimuth angles between the leading and subleading jets
p_T^{j1}	p_T of the leading jet
p_T^{j2}	p_T of the subleading jet
$p_T^{\ell_1}$	Leading lepton p_T
$p_T^{\ell\ell}$	Dilepton p_T
$z_{\ell_1}^*$	Zeppenfeld variable of the leading lepton
$z_{\ell_2}^*$	Zeppenfeld variable of the subleading lepton
p_T^{miss}	Missing transverse momentum

The nonprompt lepton backgrounds originating from leptonic decays of heavy quarks, hadrons misidentified as leptons, and electrons from photon conversion are suppressed by the identification and isolation requirements imposed on electrons and muons. The remaining contribution from the nonprompt lepton background is estimated directly from data following the technique described in Ref. [12], where the yield in a sample of data events dominated by jet production is extrapolated to the signal region using efficiencies for loosely identified leptons to pass the standard lepton selection criteria. A normalization uncertainty of 20% is assigned for the nonprompt lepton background to include possible differences in the composition of jets between the data sample used to derive these efficiencies and the data sample in the $W^\pm W^\pm$ SR [9].

Several background-enriched control regions (CRs), disjoint from one another and from the SR, are used to select event samples enriched with WZ, nonprompt lepton, tZq , and ZZ background events. The WZ CR is defined by requiring three leptons where the opposite-sign same-flavor leptons from the Z boson candidate have $p_T > 25$ and 10 GeV with the dilepton mass within 15 GeV of the nominal Z boson mass. In events with three same-flavor leptons, the opposite-sign lepton pair with the dilepton mass closest to m_Z is associated with the Z boson. The remaining lepton with $p_T > 20$ GeV is associated with the W boson. In addition, the tripleton mass $m_{\ell\ell\ell}$ is required to be greater than 100 GeV and $\max(z_{\ell_i}^*)$ must be less than 1.0. Distributions of several kinematic variables in the WZ CR are reported in Ref. [15].

The nonprompt lepton CR is defined by requiring the same selection as for the $W^\pm W^\pm$ SR, but with the b jet veto requirement inverted. The selected sample is enriched with events from the nonprompt lepton background and dominated by semileptonic $t\bar{t}$ events. Similarly, the tZq CR is defined by requiring the same selection as the WZ CR, but with the b quark veto requirement inverted. The selected sample is dominated by the tZq background process. Finally, the ZZ CR requirements select events with four leptons with the same VBS requirements as the $W^\pm W^\pm$ SR. The four CRs are used to estimate the normalization of the main background processes from data. All other background processes are estimated from simulation after applying corrections to account for small differences between data and simulation as detailed in Section 7.

To distinguish EW $W^\pm W^\pm$ production from the SM background processes before extracting the individual polarizations, a BDT is trained using the TMVA package [59]. Several discriminating observables listed in Table 3 are used as inputs to this BDT, which we will refer to as the inclusive BDT. The values of m_{jj} and $|\Delta\eta_{jj}|$ are powerful because VBS topologies typically have large values for the dijet mass and pseudorapidity separation [15]. The SM background processes are dominated by the nonprompt lepton background contribution, which comes mainly from top quark production. A large training background sample of simulated events is obtained by using oppositely charged dilepton events from top quark production.

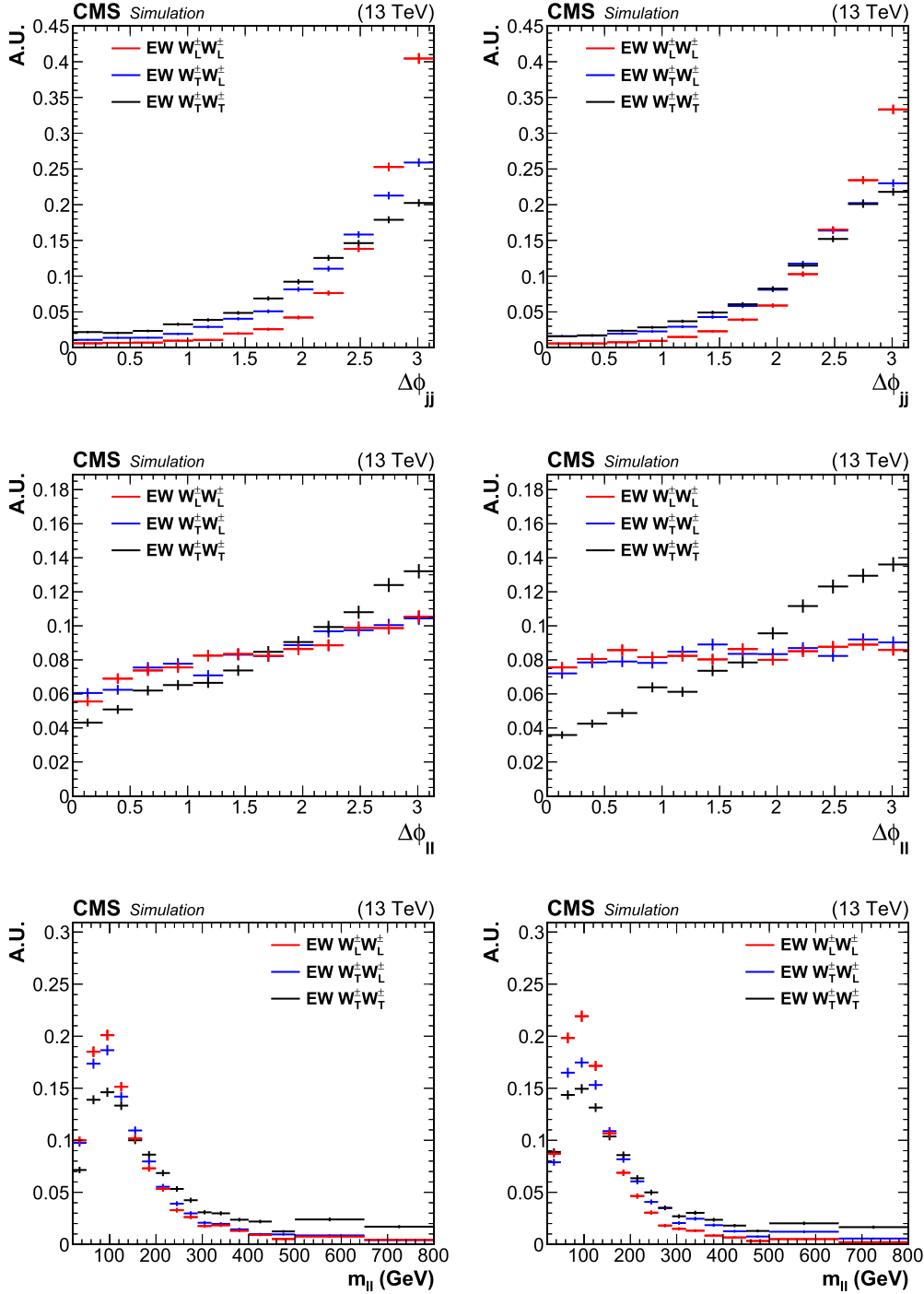


Fig. 2. Generator level distributions of $\Delta\phi_{ij}$ (upper), $\Delta\phi_{\ell\ell}$ (center), and $m_{\ell\ell}$ (lower) in the fiducial region for the $W_L^\pm W_L^\pm$, $W_L^\pm W_T^\pm$, and $W_T^\pm W_T^\pm$ processes with the helicity eigenstates defined in the parton-parton (left) and $W^\pm W^\pm$ (right) center-of-mass reference frames. The distributions are normalized to unit area. The error bars represent the uncertainties associated with the limited numbers of simulated events.

7. Systematic uncertainties

Several sources of systematic uncertainty in the cross section measurements can affect the rates and shapes of the distributions for the signal and background processes. For each source of uncertainty, the impact in different bins of the final distribution is considered as being fully correlated, whereas different sources of uncertainty are treated as uncorrelated.

The uncertainties in the integrated luminosity measurements for the data used in this analysis are 2.5, 2.3, and 2.5% for the 2016, 2017, and 2018 data samples [16–18], respectively. The to-

tal integrated luminosity has an uncertainty of 1.8% because of the uncorrelated time evolution of some systematic effects.

The simulation of pileup events assumes a total inelastic pp cross section of 69.2 mb, with an associated uncertainty of 5% [62, 63]. The impact of the pileup on the expected signal and background yields is less than 1%.

Discrepancies in the lepton reconstruction and identification efficiencies between data and simulation are adjusted by applying corrections to all MC simulation samples. The efficiency corrections, which depend on the p_T and η of the lepton, are determined using $Z \rightarrow \ell\ell$ events in the Z boson peak region [50,52]. The de-

Table 4

Systematic uncertainties of the $W_L^\pm W_L^\pm$ and $W_X^\pm W_T^\pm$, and $W_L^\pm W_X^\pm$ and $W_T^\pm W_T^\pm$ cross section measurements in units of percent.

Source of uncertainty	$W_L^\pm W_L^\pm$ (%)	$W_X^\pm W_T^\pm$ (%)	$W_L^\pm W_X^\pm$ (%)	$W_T^\pm W_T^\pm$ (%)
Integrated luminosity	3.2	1.8	1.9	1.8
Lepton measurement	3.6	1.9	2.5	1.8
Jet energy scale and resolution	11	2.9	2.5	1.1
Pileup	0.9	0.1	1.0	0.3
b tagging	1.1	1.2	1.4	1.1
Nonprompt lepton rate	17	2.7	9.3	1.6
Trigger	1.9	1.1	1.6	0.9
Limited sample size	38	3.9	14	5.7
Theory	6.8	2.3	4.0	2.3
Total systematic uncertainty	44	6.6	18	7.0
Statistical uncertainty	123	15	42	22
Total uncertainty	130	16	46	23

termination of the trigger efficiency leads to an uncertainty smaller than 1% in the expected signal yield. The lepton momentum scale uncertainty is computed by varying the momenta of the leptons in the simulation by their uncertainties, and by repeating the analysis selection. The resulting uncertainties in the event yields are about 1% for both electrons and muons. These uncertainties are treated as correlated across the three data sets.

The uncertainty in the calibration of the jet energy scale and resolution directly affects the selection efficiency of the jet multiplicity requirement and the p_T^{miss} measurement. These effects are estimated by changing the jet energy in the simulation up- and downwards by one standard deviation. The uncertainty in the jet energy scale and resolution is 2–5%, depending on the p_T and η [47], and the impact on the expected signal and background yields is 1–4%.

Discrepancies in the b tagging efficiency between data and simulation are adjusted by applying corrections to the simulated samples [57], which are estimated separately for correctly and incorrectly identified jets. Each set of values results in uncertainties in the b tagging efficiency of about 1–4%, and the impact on the expected signal and background yields is about 1%. The uncertainties in the jet energy scale and b tagging are treated as uncorrelated across the three data sets.

The dominant theoretical uncertainties corresponding to the choice of the QCD renormalization and factorization scales are estimated by varying these scales independently up and down by a factor of two from their nominal values. The largest cross section variation, while excluding the two extreme variations where one scale is varied up and the other one down, is taken as the uncertainty. The PDF uncertainties are evaluated according to the procedure described in Ref. [64]. The scale and PDF uncertainties for the processes estimated from simulation are treated as fully correlated across bins for the distributions used to extract the results. The effect of $\mathcal{O}(\alpha^7)$ correction for the unpolarized EW $W^\pm W^\pm$ process on the shapes of the distributions for the $W_L^\pm W_L^\pm$ and $W_L^\pm W_T^\pm$ processes is considered as a systematic uncertainty. The correction values are used as a symmetric shape uncertainty. The uncertainties associated with the limited numbers of simulated events and of data events used to estimate the nonprompt lepton background are also included as systematic uncertainties with the latter being the dominant contribution. A summary of the systematic uncertainties in the $W_L^\pm W_L^\pm$ and $W_X^\pm W_T^\pm$, and in the $W_L^\pm W_X^\pm$ and $W_T^\pm W_T^\pm$ cross section measurements is shown in Table 4.

8. Results

Binned maximum-likelihood fits are performed to discriminate between the signals and the remaining backgrounds using the $W^\pm W^\pm$ SR and the WZ, nonprompt lepton, tZq, and ZZ CRs. Two

Table 5

Expected yields from various SM processes and observed data events in $W^\pm W^\pm$ SR. The combination of the statistical and systematic uncertainties is shown. The expected yields are shown with their best fit normalizations from the simultaneous fit for the $W_L^\pm W_L^\pm$ and $W_X^\pm W_T^\pm$ cross sections. The $W_L^\pm W_T^\pm$ and $W_T^\pm W_T^\pm$ yields are obtained from the $W_X^\pm W_T^\pm$ yield assuming the SM prediction for the ratio of the yields. The tVx background yield includes the contributions from tV and tZq processes.

Process	Yields in $W^\pm W^\pm$ SR
$W_L^\pm W_L^\pm$	16.0 ± 18.3
$W_L^\pm W_T^\pm$	63.1 ± 10.7
$W_T^\pm W_T^\pm$	110.1 ± 18.1
QCD $W^\pm W^\pm$	13.8 ± 1.6
Interference $W^\pm W^\pm$	8.4 ± 0.6
WZ	63.3 ± 7.8
ZZ	0.7 ± 0.2
Nonprompt	213.7 ± 52.3
tVx	7.1 ± 2.2
Other background	26.9 ± 9.9
Total SM	522.9 ± 60.7
Data	524

separate fits are performed, one for the simultaneous measurements of the $W_L^\pm W_L^\pm$ and $W_X^\pm W_T^\pm$ cross sections and a second for the simultaneous measurements of the $W_L^\pm W_X^\pm$ and $W_T^\pm W_T^\pm$ cross sections. The systematic uncertainties are treated as nuisance parameters and are profiled [65,66] with the shape and normalization of each distribution varying within the respective uncertainties in the fit. The normalization uncertainties are treated as log-normal nuisance parameters. The nuisance parameters are not significantly constrained. The small QCD $W^\pm W^\pm$ contribution is normalized to the SM prediction and allowed to vary within the uncertainties. The normalizations of the tZq, ZZ, and WZ background processes are free parameters of the maximum-likelihood fits, together with the signal cross sections. A two-dimensional distribution is used in the simultaneous fits for the $W^\pm W^\pm$ SR with five bins in the inclusive BDT and five bins in the corresponding signal BDT. The m_{jj} distribution is used for the CRs in the fit with four bins. The bin boundaries are chosen to have similar $W_L^\pm W_L^\pm$ and $W_L^\pm W_X^\pm$ contributions across the bins.

The interference contributions between the EW and QCD diagrams for the $W^\pm W^\pm$ and WZ processes are normalized to the SM predictions within the uncertainties. The impact of treatment of the interference contributions on the results is evaluated by performing a set of alternative fits where the interference contributions between the EW diagrams for the $W_L^\pm W_L^\pm$ and $W_X^\pm W_T^\pm$ or $W_L^\pm W_X^\pm$ and $W_T^\pm W_T^\pm$ processes and QCD diagrams are scaled with the square root of the measured to the predicted cross section ratios. The two approaches yield consistent results.

The distributions of m_{jj} (upper left), $\Delta\phi_{jj}$ (upper right), $\Delta\phi_{\ell\ell}$ (lower left), and the output score of the inclusive BDT (lower right) in the $W^\pm W^\pm$ SR are shown in Fig. 3. The distributions of the two signal BDT output scores are shown in Fig. 4. The predicted yields are shown with their best fit normalizations from the simultaneous fit for the $W_L^\pm W_L^\pm$ and $W_X^\pm W_T^\pm$ cross sections. The data yields, together with the SM expectations with the best fit normalizations, are given in Table 5. The background yields with the best fit normalizations from the simultaneous fit for the $W_L^\pm W_X^\pm$ and $W_T^\pm W_T^\pm$ cross sections are consistent with the yields shown in Table 5 within a few percent.

The fiducial region for the cross section measurements is defined by requiring two same-sign leptons (electrons or muons) with $p_T > 20$ GeV, $|\eta| < 2.5$, and $m_{\ell\ell} > 20$ GeV, and two jets with $m_{jj} > 500$ GeV and $|\Delta\eta_{jj}| > 2.5$. The leptons at the generator level are selected at the so-called dressed level by combining the four-

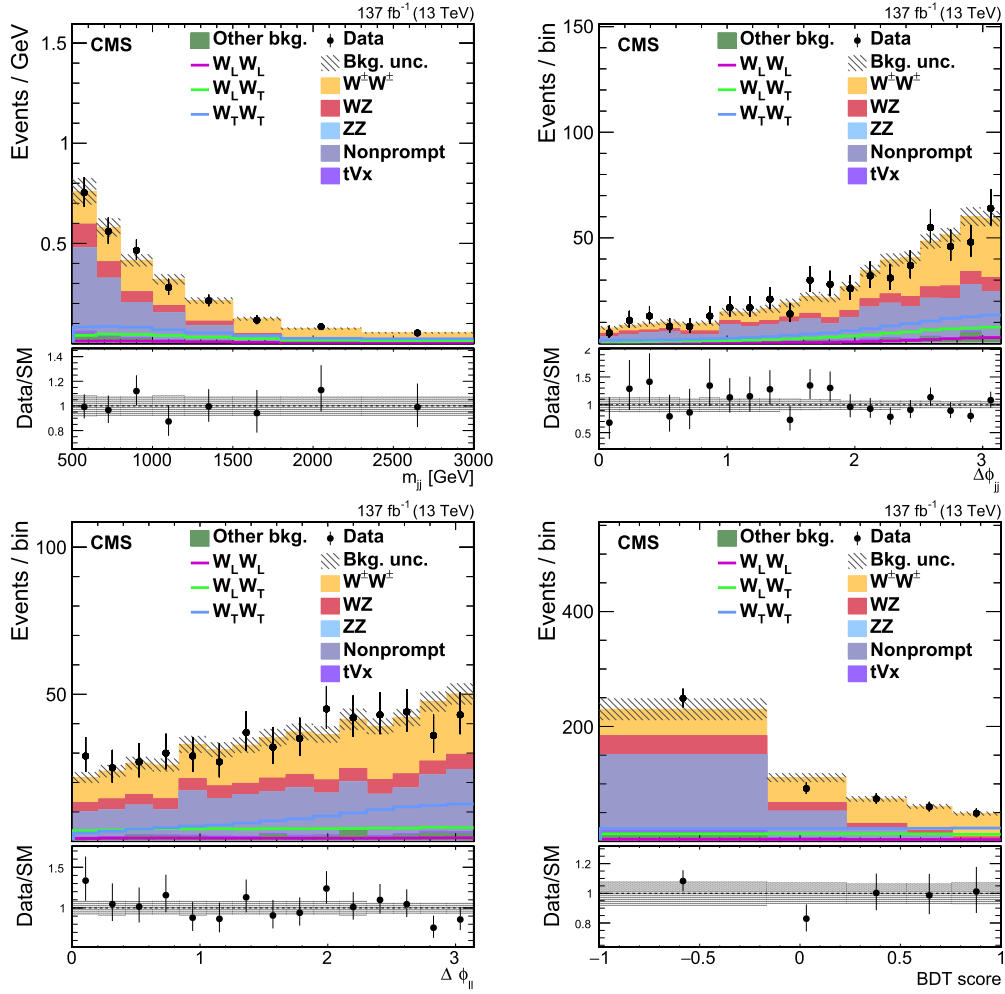


Fig. 3. Distributions of the m_{jj} (upper left), $\Delta\phi_{jj}$ (upper right), $\Delta\phi_{\ell\ell}$ (lower left), and of the output score of the inclusive BDT (lower right) in the $W^\pm W^\pm$ SR. The predicted yields are shown with their best fit normalizations from the simultaneous fit. The histograms for the $W^\pm W^\pm$ process include the contributions from the $W_L^\pm W_L^\pm$, $W_L^\pm W_T^\pm$, and $W_T^\pm W_T^\pm$ processes (shown separately as solid lines), QCD $W^\pm W^\pm$, and interference. The histograms for other backgrounds include the contributions from double parton scattering, VVV, and from oppositely charged dilepton final states from $t\bar{t}$, tW , W^+W^- , and Drell-Yan processes. The overflow is included in the last bin. The bottom panel in each figure shows the ratio of the number of events observed in data to that of the total SM prediction. The gray bands represent the uncertainties in the predicted yields. The vertical bars represent the statistical uncertainties in the data.

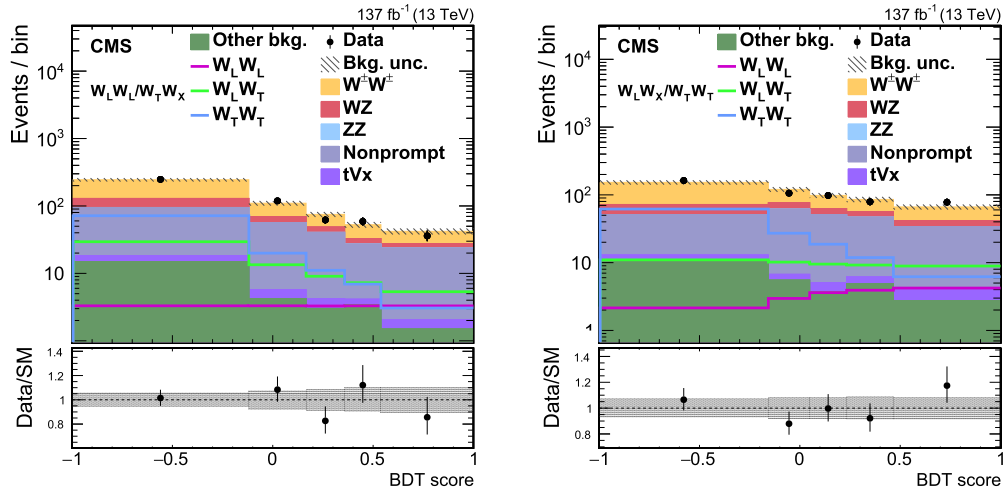


Fig. 4. Distributions of the output score of the signal BDT used for the $W_L^\pm W_L^\pm$ and $W_T^\pm W_T^\pm$ cross section measurements (left) and of the output score of the signal BDT used for the $W_L^\pm W_T^\pm$ and $W_T^\pm W_T^\pm$ cross section measurements (right). The predicted yields are shown with their best fit normalizations from the simultaneous fit. The histograms for the $W^\pm W^\pm$ process include the contributions from the $W_L^\pm W_L^\pm$, $W_L^\pm W_T^\pm$, and $W_T^\pm W_T^\pm$ processes (shown separately as solid lines), QCD $W^\pm W^\pm$, and interference. The histograms for other backgrounds include the contributions from double parton scattering, VVV, and from oppositely charged dilepton final states from $t\bar{t}$, tW , W^+W^- , and Drell-Yan processes. The bottom panel in each figure shows the ratio of the number of events observed in data to that of the total SM prediction. The gray bands represent the uncertainties in the predicted yields. The vertical bars represent the statistical uncertainties in the data.

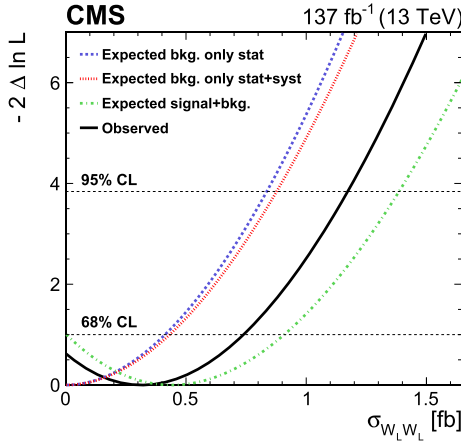


Fig. 5. Profile likelihood scan as a function of the $W_L^+ W_L^+$ cross section. The red (blue) line represents the expected values in the background-only hypothesis, i.e., assuming no contribution from the $W_L^+ W_L^+$ process, considering all systematic uncertainties (only statistical ones). The green line shows the expected values for the signal-plus-background hypothesis. The observed values are represented by the black line.

Table 6

Measured fiducial cross sections for the $W_L^+ W_L^+$ and $W_X^+ W_T^+$ processes, and for the $W_L^+ W_X^+$ and $W_T^+ W_T^+$ processes for the helicity eigenstates defined in the $W^\pm W^\pm$ center-of-mass frame. The combination of the statistical and systematic uncertainties is shown. The theoretical predictions including the $\mathcal{O}(\alpha_s \alpha^6)$ and $\mathcal{O}(\alpha^7)$ corrections to the MADGRAPH5_amc@NLO LO cross sections, as described in the text, are also shown. The theoretical uncertainties include statistical, PDF, and LO scale uncertainties; \mathcal{B} is the branching fraction for $WW \rightarrow \ell\nu\ell'\nu$ [55].

Process	$\sigma \mathcal{B}$ (fb)	Theoretical prediction (fb)
$W_L^+ W_L^+$	$0.32^{+0.42}_{-0.40}$	0.44 ± 0.05
$W_X^+ W_T^+$	$3.06^{+0.51}_{-0.48}$	3.13 ± 0.35
$W_L^+ W_X^+$	$1.20^{+0.56}_{-0.53}$	1.63 ± 0.18
$W_T^+ W_T^+$	$2.11^{+0.49}_{-0.47}$	1.94 ± 0.21

momentum of each lepton after final-state photon radiation with that of photons found within a cone of $\Delta R = 0.1$ around the lepton. The jets at generator level are clustered from stable particles, excluding neutrinos, using the anti- k_T clustering algorithm with a distance parameter of 0.4, and are required to satisfy $p_T > 50$ GeV and $|\eta| < 4.7$. Jets within $\Delta R < 0.4$ of the selected charged leptons are not included. The overall signal selection efficiency within the fiducial region is about 40%. Electrons and muons produced in the decay of a τ lepton are not included in the definition of the fiducial region. Nonfiducial signal events, i.e., events selected at the reconstructed level that do not satisfy the fiducial requirements, are scaled together with the fiducial signal events in the simultaneous fit. The relative contribution of the nonfiducial events is approximately 20%. The nonfiducial events are treated as background processes.

The fit results for the $W_L^+ W_L^+$ and $W_X^+ W_T^+$ cross sections are shown in Fig. 5 as scans of the negative profile log-likelihood, $-2\Delta \ln \mathcal{L}$, as a function of the $W_L^+ W_L^+$ cross section. The expected distributions include the contribution from the $W_X^+ W_T^+$ process. The corresponding observed (expected) upper limit at 95% confidence level (CL) is 1.17 (0.88) fb. The fiducial cross section measurements for the $W_L^+ W_L^+$ and $W_X^+ W_T^+$ processes and the theoretical predictions are shown in Table 6. The measured cross section values agree with the theoretical predictions within uncertainties.

The fiducial cross section measurements for the $W_L^+ W_X^+$ and $W_T^+ W_T^+$ processes are extracted from a separate fit including the corresponding signal BDT. The measurements and the theoretical predictions are summarized in Table 6. The significance of the measured $W_L^+ W_X^+$ yield is quantified using background-only hy-

Table 7

Measured fiducial cross sections for the $W_L^+ W_L^+$ and $W_X^+ W_T^+$ processes, and for the $W_L^+ W_X^+$ and $W_T^+ W_T^+$ processes for the helicity eigenstates defined in the parton-parton center-of-mass frame. The combination of the statistical and systematic uncertainties is shown. The theoretical predictions including the $\mathcal{O}(\alpha_s \alpha^6)$ and $\mathcal{O}(\alpha^7)$ corrections to the MADGRAPH5_amc@NLO LO cross sections, as described in the text, are also shown. The theoretical uncertainties include statistical, PDF, and LO scale uncertainties; \mathcal{B} is the branching fraction for $WW \rightarrow \ell\nu\ell'\nu$ [55].

Process	$\sigma \mathcal{B}$ (fb)	Theoretical prediction (fb)
$W_L^+ W_L^+$	$0.24^{+0.40}_{-0.37}$	0.28 ± 0.03
$W_X^+ W_T^+$	$3.25^{+0.50}_{-0.48}$	3.32 ± 0.37
$W_L^+ W_X^+$	$1.40^{+0.60}_{-0.57}$	1.71 ± 0.19
$W_T^+ W_T^+$	$2.03^{+0.51}_{-0.50}$	1.89 ± 0.21

pothesis, i.e., assuming no contribution from the $W_L^+ W_X^+$ process, under the asymptotic approximation [67] and corresponds to 2.3 standard deviations. The expected significance is evaluated with an Asimov data set [67] and corresponds to 3.1 standard deviations.

The measurements are also performed for the polarized observables defined using the helicity eigenstates in the initial state parton-parton center-of-mass reference frame. Defining the polarization vectors in the parton-parton center-of-mass reference frame changes the respective contributions of $W_L^+ W_L^+$, $W_L^+ W_X^+$ and $W_X^+ W_T^+$, and the distributions of the input observables sensitive to the polarization [68]. The fiducial cross section measurements and the theoretical predictions are summarized in Table 7. The observed (expected) 95% CL upper limit of the production cross section is 1.06 (0.85) fb for the $W_L^+ W_L^+$ process. The observed (expected) significance of the $W_L^+ W_X^+$ process is 2.6 (2.9) standard deviations.

9. Summary

The first measurements of production cross sections for polarized same-sign $W^\pm W^\pm$ boson pairs are reported. The measurements are based on a sample of proton-proton collisions at a center-of-mass energy of 13 TeV collected by the CMS detector at the LHC, corresponding to an integrated luminosity of 137 fb^{-1} . Events are selected by requiring exactly two same-sign leptons (electrons or muons), moderate missing transverse momentum, and two jets with a large rapidity separation and a high dijet mass. Boosted decision trees are used to separate between the polarized scattering processes by exploiting the kinematic differences. An observed (expected) 95% confidence level upper limit on the production cross section for longitudinally polarized same-sign $W^\pm W^\pm$ boson pairs of 1.17 (0.88) fb is reported with the helicity eigenstates defined in the $W^\pm W^\pm$ center-of-mass reference frame. The electroweak production of the $W^\pm W^\pm$ boson pairs where at least one of the W bosons is longitudinally polarized is measured with an observed (expected) significance of 2.3 (3.1) standard deviations. Results are also reported with the polarizations defined in the parton-parton center-of-mass reference frame. The measured cross section values agree with the standard model predictions.

Declaration of competing interest

The authors declare that they have no known competing financial interests or personal relationships that could have appeared to influence the work reported in this paper.

Acknowledgements

We congratulate our colleagues in the CERN accelerator departments for the excellent performance of the LHC and thank the technical and administrative staffs at CERN and at other CMS institutes for their contributions to the success of the CMS effort.

In addition, we gratefully acknowledge the computing centers and personnel of the Worldwide LHC Computing Grid for delivering so effectively the computing infrastructure essential to our analyses. Finally, we acknowledge the enduring support for the construction and operation of the LHC and the CMS detector provided by the following funding agencies: BMBWF and FWF (Austria); FNRS and FWO (Belgium); CNPq, CAPES, FAPERJ, FAPERGS, and FAPESP (Brazil); MES (Bulgaria); CERN; CAS, MOST, and NSFC (China); COLCIENCIAS (Colombia); MSES and CSF (Croatia); RIF (Cyprus); SENESCYT (Ecuador); MoER, ERC IUT, PUT and ERDF (Estonia); Academy of Finland, MEC, and HIP (Finland); CEA and CNRS/IN2P3 (France); BMBF, DFG, and HGF (Germany); GSRT (Greece); NK-FIA (Hungary); DAE and DST (India); IPM (Iran); SFI (Ireland); INFN (Italy); MSIP and NRF (Republic of Korea); MES (Latvia); LAS (Lithuania); MOE and UM (Malaysia); BUAP, CINVESTAV, CONACYT, LNS, SEP, and UASLP-FAI (Mexico); MOS (Montenegro); MBIE (New Zealand); PAEC (Pakistan); MSHE and NSC (Poland); FCT (Portugal); JINR (Dubna); MON, ROSATOM, RAS, RFBR, and NRC KI (Russia); MESTD (Serbia); SEIDI, CPAN, PCTI, and FEDER (Spain); MoSTR (Sri Lanka); Swiss Funding Agencies (Switzerland); MST (Taipei); ThEPCenter, IPST, STAR, and NSTDA (Thailand); TUBITAK and TAEK (Turkey); NASU (Ukraine); STFC (United Kingdom); DOE and NSF (USA).

Individuals have received support from the Marie-Curie program and the European Research Council and Horizon 2020 Grant, contract Nos. 675440, 752730, and 765710 (European Union); the Leventis Foundation; the Alfred P. Sloan Foundation; the Alexander von Humboldt Foundation; the Belgian Federal Science Policy Office; the Fonds pour la Formation à la Recherche dans l'Industrie et dans l'Agriculture (FRIA-Belgium); the Agentschap voor Innovatie door Wetenschap en Technologie (IWT-Belgium); the F.R.S. - FNRS and FWO (Belgium) under the "Excellence of Science - EOS" - be.h project n. 30820817; the Beijing Municipal Science and Technology Commission, No. Z191100007219010; the Ministry of Education, Youth and Sports (MEYS) of the Czech Republic; the Deutsche Forschungsgemeinschaft (DFG) under Germany's Excellence Strategy - EXC 2121 "Quantum Universe" - 390833306; the Lendület ("Momentum") Program and the János Bolyai Research Scholarship of the Hungarian Academy of Sciences, the New National Excellence Program ÚNKP, the NK-FIA research grants 123842, 123959, 124845, 124850, 125105, 128713, 128786, and 129058 (Hungary); the Council of Science and Industrial Research, India; the HOMING PLUS program of the Foundation for Polish Science, cofinanced from European Union, Regional Development Fund, the Mobility Plus program of the Ministry of Science and Higher Education, the National Science Center (Poland), contracts Harmonia 2014/14/M/ST2/00428, Opus 2014/13/B/ST2/02543, 2014/15/B/ST2/03998, and 2015/19/B/ST2/02861, Sonata-bis 2012/07/E/ST2/01406; the National Priorities Research Program by Qatar National Research Fund; the Ministry of Science and Higher Education, project no. 02.a03.21.0005 (Russia); the Tomsk Polytechnic University Competitiveness Enhancement Program; the Programa Estatal de Fomento de la Investigación Científica y Técnica de Excelencia María de Maeztu, grant MDM-2015-0509 and the Programa Severo Ochoa del Principado de Asturias; the Thalís and Aristeia programs cofinanced by EU-ESF and the Greek NSRF; the Rachadapisek Sompot Fund for Postdoctoral Fellowship, Chulalongkorn University and the Chulalongkorn Academic into Its 2nd Century Project Advancement Project (Thailand); the Kavli Foundation; the Nvidia Corporation; the SuperMicro Corporation; the Welch Foundation, contract C-1845; and the Weston Havens Foundation (USA).

References

- [1] B.W. Lee, C. Quigg, H.B. Thacker, The strength of weak interactions at very high-energies and the Higgs boson mass, *Phys. Rev. Lett.* 38 (1977) 883, <https://doi.org/10.1103/PhysRevLett.38.883>.
- [2] B.W. Lee, C. Quigg, H.B. Thacker, Weak interactions at very high-energies: the role of the Higgs boson mass, *Phys. Rev. D* 16 (1977) 1519, <https://doi.org/10.1103/PhysRevD.16.1519>.
- [3] ATLAS Collaboration, Observation of a new particle in the search for the standard model Higgs boson with the ATLAS detector at the LHC, *Phys. Lett. B* 716 (2012) 1, <https://doi.org/10.1016/j.physletb.2012.08.020>, arXiv:1207.7214.
- [4] CMS Collaboration, Observation of a new boson at a mass of 125 GeV with the CMS experiment at the LHC, *Phys. Lett. B* 716 (2012) 30, <https://doi.org/10.1016/j.physletb.2012.08.021>, arXiv:1207.7235.
- [5] CMS Collaboration, Observation of a new boson with mass near 125 GeV in pp collisions at $\sqrt{s} = 7$ and 8 TeV, *J. High Energy Phys.* 06 (2013) 081, [https://doi.org/10.1007/JHEP06\(2013\)081](https://doi.org/10.1007/JHEP06(2013)081), arXiv:1303.4571.
- [6] D. Espriu, B. Yencho, Longitudinal WW scattering in light of the Higgs boson discovery, *Phys. Rev. D* 87 (2013) 055017, <https://doi.org/10.1103/PhysRevD.87.055017>, arXiv:1212.4158.
- [7] J. Chang, K. Cheung, C.-T. Lu, T.-C. Yuan, WW scattering in the era of post-Higgs-boson discovery, *Phys. Rev. D* 87 (2013) 093005, <https://doi.org/10.1103/PhysRevD.87.093005>, arXiv:1303.6335.
- [8] G. Aad, et al., ATLAS, CMS, Measurements of the Higgs boson production and decay rates and constraints on its couplings from a combined ATLAS and CMS analysis of the LHC pp collision data at $\sqrt{s} = 7$ and 8 TeV, *J. High Energy Phys.* 08 (2016) 045, [https://doi.org/10.1007/JHEP08\(2016\)045](https://doi.org/10.1007/JHEP08(2016)045), arXiv:1606.02266.
- [9] CMS Collaboration, Measurements of properties of the Higgs boson decaying to a W boson pair in pp collisions at $\sqrt{s} = 13$ TeV, *Phys. Lett. B* 791 (2019) 96, <https://doi.org/10.1016/j.physletb.2018.12.073>, arXiv:1806.05246.
- [10] S. Brass, C. Fleper, W. Kilian, J. Reuter, M. Sekulla, Transversal modes and Higgs bosons in electroweak vector-boson scattering at the LHC, *Eur. Phys. J. C* 78 (2018) 931, <https://doi.org/10.1140/epjc/s10052-018-6398-4>, arXiv:1807.02512.
- [11] ATLAS Collaboration, Evidence for electroweak production of $W^{\pm}W^{\pm}jj$ in pp collisions at $\sqrt{s} = 8$ TeV with the ATLAS detector, *Phys. Rev. Lett.* 113 (2014) 141803, <https://doi.org/10.1103/PhysRevLett.113.141803>, arXiv:1405.6241.
- [12] CMS Collaboration, Study of vector boson scattering and search for new physics in events with two same-sign leptons and two jets, *Phys. Rev. Lett.* 114 (2015) 051801, <https://doi.org/10.1103/PhysRevLett.114.051801>, arXiv:1410.6315.
- [13] CMS Collaboration, Observation of electroweak production of same-sign W boson pairs in the two jet and two same-sign lepton final state in proton-proton collisions at $\sqrt{s} = 13$ TeV, *Phys. Rev. Lett.* 120 (2018) 081801, <https://doi.org/10.1103/PhysRevLett.120.081801>, arXiv:1709.05822.
- [14] ATLAS Collaboration, Observation of electroweak production of a same-sign W boson pair in association with two jets in pp collisions at $\sqrt{s} = 13$ TeV with the ATLAS detector, *Phys. Rev. Lett.* 123 (2019) 161801, <https://doi.org/10.1103/PhysRevLett.123.161801>, arXiv:1906.03203.
- [15] CMS Collaboration, Measurements of production cross sections of WZ and same-sign WW boson pairs in association with two jets in proton-proton collisions at $\sqrt{s} = 13$ TeV, *Phys. Lett. B* 809 (2020) 135710, <https://doi.org/10.1016/j.physletb.2020.135710>, arXiv:2005.01173.
- [16] CMS Collaboration, CMS luminosity measurement for the 2016 data-taking period, CMS Physics Analysis Summary CMS-PAS-LUM-17-001, <https://cds.cern.ch/record/2138682>, 2017.
- [17] CMS Collaboration, CMS luminosity measurement for the 2017 data-taking period at $\sqrt{s} = 13$ TeV, CMS Physics Analysis Summary CMS-PAS-LUM-17-004, <https://cds.cern.ch/record/2621960>, 2017.
- [18] CMS Collaboration, CMS luminosity measurement for the 2018 data-taking period at $\sqrt{s} = 13$ TeV, CMS Physics Analysis Summary CMS-PAS-LUM-18-002, <https://cds.cern.ch/record/2676164>, 2018.
- [19] CMS Collaboration, The CMS experiment at the CERN LHC, *J. Instrum.* 3 (2008) S08004, <https://doi.org/10.1088/1748-0221/3/08/S08004>.
- [20] CMS Collaboration, The CMS trigger system, *J. Instrum.* 12 (2017) P01020, <https://doi.org/10.1088/1748-0221/12/01/P01020>, arXiv:1609.02366.
- [21] S. Agostinelli, et al., GEANT4, GEANT4 - a simulation toolkit, *Nucl. Instrum. Methods A* 506 (2003) 250, [https://doi.org/10.1016/S0168-9002\(03\)01368-8](https://doi.org/10.1016/S0168-9002(03)01368-8).
- [22] R. Frederix, S. Frixione, Merging meets matching in MC@NLO, *J. High Energy Phys.* 12 (2012) 061, [https://doi.org/10.1007/JHEP12\(2012\)061](https://doi.org/10.1007/JHEP12(2012)061), arXiv:1209.6215.
- [23] J. Alwall, R. Frederix, S. Frixione, V. Hirschi, F. Maltoni, O. Mattelaer, H.S. Shao, T. Stelzer, P. Torrielli, M. Zaro, The automated computation of tree-level and next-to-leading order differential cross sections, and their matching to parton shower simulations, *J. High Energy Phys.* 07 (2014) 079, [https://doi.org/10.1007/JHEP07\(2014\)079](https://doi.org/10.1007/JHEP07(2014)079), arXiv:1405.0301.
- [24] D. Buarque Franzosi, O. Mattelaer, R. Ruiz, S. Shil, Automated predictions from polarized matrix elements, *J. High Energy Phys.* 04 (2020) 082, [https://doi.org/10.1007/JHEP04\(2020\)082](https://doi.org/10.1007/JHEP04(2020)082), arXiv:1912.01725.
- [25] R.D. Ball, et al., NNPDF, Parton distributions from high-precision collider data, *Eur. Phys. J. C* 77 (2017) 663, <https://doi.org/10.1140/epjc/s10052-017-5199-5>, arXiv:1706.00428.

- [26] A. Ballestrero, A. Belhouari, G. Bevilacqua, V. Kashkan, E. Maina, PHANTOM: a Monte Carlo event generator for six parton final states at high energy colliders, *Comput. Phys. Commun.* 180 (2009) 401, <https://doi.org/10.1016/j.cpc.2008.10.005>, arXiv:0801.3359.
- [27] A. Ballestrero, D. Buarque Franzosi, L. Oggero, E. Maina, Vector boson scattering at the LHC: counting experiments for unitarized models in a full six fermion approach, *J. High Energy Phys.* 03 (2012) 031, [https://doi.org/10.1007/JHEP03\(2012\)031](https://doi.org/10.1007/JHEP03(2012)031), arXiv:1112.1171.
- [28] A. Ballestrero, E. Maina, G. Pelliccioli, W boson polarization in vector boson scattering at the LHC, *J. High Energy Phys.* 03 (2018) 170, [https://doi.org/10.1007/JHEP03\(2018\)170](https://doi.org/10.1007/JHEP03(2018)170), arXiv:1710.09339.
- [29] B. Biedermann, A. Denner, M. Pellen, Large electroweak corrections to vector boson scattering at the Large Hadron Collider, *Phys. Rev. Lett.* 118 (2017) 261801, <https://doi.org/10.1103/PhysRevLett.118.261801>, arXiv:1611.02951.
- [30] B. Biedermann, A. Denner, M. Pellen, Complete NLO corrections to W^+W^+ scattering and its irreducible background at the LHC, *J. High Energy Phys.* 10 (2017) 124, [https://doi.org/10.1007/JHEP10\(2017\)124](https://doi.org/10.1007/JHEP10(2017)124), arXiv:1708.00268.
- [31] A. Denner, S. Pozzorini, One loop leading logarithms in electroweak radiative corrections. 1. Results, *Eur. Phys. J. C* 18 (2001) 461, <https://doi.org/10.1007/s100520100551>, arXiv:hep-ph/0010201.
- [32] J. Alwall, S. Höche, F. Krauss, N. Lavesson, L. Lönnblad, F. Maltoni, M.L. Mangano, M. Moretti, C.G. Papadopoulos, F. Piccinini, S. Schumann, M. Treccani, J. Winter, M. Worek, Comparative study of various algorithms for the merging of parton showers and matrix elements in hadronic collisions, *Eur. Phys. J. C* 53 (2008) 473, <https://doi.org/10.1140/epjc/s10052-007-0490-5>, arXiv:0706.2569.
- [33] S. Frixione, B.R. Webber, Matching NLO QCD computations and parton shower simulations, *J. High Energy Phys.* 06 (2002) 029, <https://doi.org/10.1088/1126-6708/2002/06/029>, arXiv:hep-ph/0204244.
- [34] P. Nason, A new method for combining NLO QCD with shower Monte Carlo algorithms, *J. High Energy Phys.* 11 (2004) 040, <https://doi.org/10.1088/1126-6708/2004/11/040>, arXiv:hep-ph/0409146.
- [35] S. Frixione, P. Nason, C. Oleari, Matching NLO QCD computations with parton shower simulations: the POWHEG method, *J. High Energy Phys.* 11 (2007) 070, <https://doi.org/10.1088/1126-6708/2007/11/070>, arXiv:0709.2092.
- [36] S. Alioli, P. Nason, C. Oleari, E. Re, NLO vector-boson production matched with shower in POWHEG, *J. High Energy Phys.* 07 (2008) 060, <https://doi.org/10.1088/1126-6708/2008/07/060>, arXiv:0805.4802.
- [37] S. Alioli, P. Nason, C. Oleari, E. Re, A general framework for implementing NLO calculations in shower Monte Carlo programs: the POWHEG BOX, *J. High Energy Phys.* 06 (2010) 043, [https://doi.org/10.1007/JHEP06\(2010\)043](https://doi.org/10.1007/JHEP06(2010)043), arXiv:1002.2581.
- [38] CMS Collaboration, Measurement of the associated production of a single top quark and a Z boson in pp collisions at $\sqrt{s} = 13$ TeV, *Phys. Lett. B* 779 (2018) 358, <https://doi.org/10.1016/j.physletb.2018.02.025>, arXiv:1712.02825.
- [39] T. Sjöstrand, S. Ask, J.R. Christiansen, R. Corke, N. Desai, P. Ilten, S. Mrenna, S. Prestel, C.O. Rasmussen, P.Z. Skands, An introduction to PYTHIA 8.2, *Comput. Phys. Commun.* 191 (2015) 159, <https://doi.org/10.1016/j.cpc.2015.01.024>, arXiv:1410.3012.
- [40] R.D. Ball, et al., NNPDF, Parton distributions for the LHC Run II, *J. High Energy Phys.* 04 (2015) 040, [https://doi.org/10.1007/JHEP04\(2015\)040](https://doi.org/10.1007/JHEP04(2015)040), arXiv:1410.8849.
- [41] P. Skands, S. Carrazza, J. Rojo, Tuning PYTHIA 8.1: the Monash 2013 tune, *Eur. Phys. J. C* 74 (2014) 3024, <https://doi.org/10.1140/epjc/s10052-014-3024-y>, arXiv:1404.5630.
- [42] CMS Collaboration, Event generator tunes obtained from underlying event and multiparton scattering measurements, *Eur. Phys. J. C* 76 (2016) 155, <https://doi.org/10.1140/epjc/s10052-016-3988-x>, arXiv:1512.00815.
- [43] CMS Collaboration, Extraction and validation of a new set of CMS PYTHIA8 tunes from underlying-event measurements, *Eur. Phys. J. C* 80 (2020) 4, <https://doi.org/10.1140/epjc/s10052-019-7499-4>, arXiv:1903.12179.
- [44] CMS Collaboration, Particle-flow reconstruction and global event description with the CMS detector, *J. Instrum.* 12 (2017) P10003, <https://doi.org/10.1088/1748-0221/12/10/P10003>, arXiv:1706.04965.
- [45] M. Cacciari, G.P. Salam, G. Soyez, The anti- k_T jet clustering algorithm, *J. High Energy Phys.* 04 (2008) 063, <https://doi.org/10.1088/1126-6708/2008/04/063>, arXiv:0802.1189.
- [46] M. Cacciari, G.P. Salam, G. Soyez, FastJet user manual, *Eur. Phys. J. C* 72 (2012) 1896, <https://doi.org/10.1140/epjc/s10052-012-1896-2>, arXiv:1111.6097.
- [47] CMS Collaboration, Jet energy scale and resolution in the CMS experiment in pp collisions at 8 TeV, *J. Instrum.* 12 (2017) P02014, <https://doi.org/10.1088/1748-0221/12/02/P02014>, arXiv:1607.03663.
- [48] CMS Collaboration, Pileup mitigation at CMS in 13 TeV data, *J. Instrum.* 15 (2020) P09018, <https://doi.org/10.1088/1748-0221/15/09/P09018>, arXiv:2003.00503.
- [49] CMS Collaboration, Performance of missing transverse momentum reconstruction in proton-proton collisions at $\sqrt{s} = 13$ TeV using the CMS detector, *J. Instrum.* 14 (2019) P07004, <https://doi.org/10.1088/1748-0221/14/07/P07004>, arXiv:1903.06078.
- [50] CMS Collaboration, Performance of electron reconstruction and selection with the CMS detector in proton-proton collisions at $\sqrt{s} = 8$ TeV, *J. Instrum.* 10 (2015) P06005, <https://doi.org/10.1088/1748-0221/10/06/P06005>, arXiv:1502.02701.
- [51] CMS Collaboration, Electron and photon performance in CMS with the full 2017 data sample and additional 2016 highlights for the CALOR 2018 Conference, CMS Detector Performance Summary CMS-DP-2018-017, <https://cds.cern.ch/record/2320638>, 2018.
- [52] CMS Collaboration, Performance of the CMS muon detector and muon reconstruction with proton-proton collisions at $\sqrt{s} = 13$ TeV, *J. Instrum.* 13 (2018) P06015, <https://doi.org/10.1088/1748-0221/13/06/P06015>, arXiv:1804.04528.
- [53] CMS Collaboration, Performance of CMS muon reconstruction in cosmic-ray events, *J. Instrum.* 5 (2010) T03022, <https://doi.org/10.1088/1748-0221/5/03/T03022>, arXiv:0911.4994.
- [54] CMS Collaboration, Performance of the reconstruction and identification of high-momentum muons in proton-proton collisions at $\sqrt{s} = 13$ TeV, *J. Instrum.* 15 (2020) P02027, <https://doi.org/10.1088/1748-0221/15/02/P02027>, arXiv:1912.03516.
- [55] Particle Data Group, P.A. Zyla, et al., Review of particle physics, *Prog. Theor. Exp. Phys.* 2020 (2020) 083C01, <https://doi.org/10.1093/ptep/ptaa104>.
- [56] D.L. Rainwater, R. Szalapski, D. Zeppenfeld, Probing color singlet exchange in Z + 2-jet events at the CERN LHC, *Phys. Rev. D* 54 (1996) 6680, <https://doi.org/10.1103/PhysRevD.54.6680>, arXiv:hep-ph/9605444.
- [57] CMS Collaboration, Identification of heavy-flavour jets with the CMS detector in pp collisions at 13 TeV, *J. Instrum.* 13 (2018) P05011, <https://doi.org/10.1088/1748-0221/13/05/P05011>, arXiv:1712.07158.
- [58] K. Doroba, J. Kalinowski, J. Kuczumski, S. Pokorski, J. Rosiek, M. Szeleper, S. Tkaczyk, The $W_L W_L$ scattering at the LHC: improving the selection criteria, *Phys. Rev. D* 86 (2012) 036011, <https://doi.org/10.1103/PhysRevD.86.036011>, arXiv:1201.2768.
- [59] H. Voss, A. Höcker, J. Stelzer, F. Tegenfeldt, TMVA, the toolkit for multivariate data analysis with ROOT, in: *Xlth International Workshop on Advanced Computing and Analysis Techniques in Physics Research (ACAT)*, 2007, p. 40, arXiv:physics/0703039 [PoS(ACAT)040].
- [60] F. Chollet, et al., Keras, <https://keras.io>, 2015.
- [61] M. Abadi, et al., Tensorflow: large-scale machine learning on heterogeneous distributed systems, <http://tensorflow.org>, 2016, software available from tensorflow.org.
- [62] ATLAS Collaboration, Measurement of the inelastic proton-proton cross section at $\sqrt{s} = 13$ TeV with the ATLAS detector at the LHC, *Phys. Rev. Lett.* 117 (2016) 182002, <https://doi.org/10.1103/PhysRevLett.117.182002>, arXiv:1606.02625.
- [63] CMS Collaboration, Measurement of the inelastic proton-proton cross section at $\sqrt{s} = 13$ TeV, *J. High Energy Phys.* 07 (2018) 161, [https://doi.org/10.1007/JHEP07\(2018\)161](https://doi.org/10.1007/JHEP07(2018)161), arXiv:1802.02613.
- [64] J. Butterworth, S. Carrazza, A. Cooper-Sarkar, A. De Roeck, J. Feltesse, J. Forte, Stefano Gao, S. Glazov, J. Huston, Z. Kassabov, PDF4LHC recommendations for LHC Run II, *J. Phys. G* 43 (2016) 023001, <https://doi.org/10.1088/0954-3899/43/2/023001>, arXiv:1510.03865.
- [65] T. Junk, Confidence level computation for combining searches with small statistics, *Nucl. Instrum. Methods A* 434 (1999) 435, [https://doi.org/10.1016/S0168-9002\(99\)00498-2](https://doi.org/10.1016/S0168-9002(99)00498-2), arXiv:hep-ex/9902006.
- [66] A.L. Read, Presentation of search results: the CL_s technique, *J. Phys. G* 28 (2002) 2693, <https://doi.org/10.1088/0954-3899/28/10/313>.
- [67] G. Cowan, K. Cranmer, E. Gross, O. Vitells, Asymptotic formulae for likelihood-based tests of new physics, *Eur. Phys. J. C* 71 (2011) 1554, <https://doi.org/10.1140/epjc/s10052-011-1554-0>, arXiv:1007.1727, <https://doi.org/10.1140/epjc/s10052-013-2501-z> (Erratum).
- [68] A. Ballestrero, E. Maina, G. Pelliccioli, Different polarization definitions in same-sign WW scattering at the LHC, *Phys. Lett. B* 810 (2020) 135856, <https://doi.org/10.1016/j.physletb.2020.135856>, arXiv:2007.07133.

The CMS Collaboration

A.M. Sirunyan[†], A. Tumasyan

Yerevan Physics Institute, Yerevan, Armenia

W. Adam, T. Bergauer, M. Dragicevic, J. Erö, A. Escalante Del Valle, R. Frühwirth¹, M. Jeitler¹, N. Krammer, L. Lechner, D. Liko, I. Mikulec, F.M. Pitters, N. Rad, J. Schieck¹, R. Schöfbeck, M. Spanring, S. TEMPL, W. Waltenberger, C.-E. Wulz¹, M. Zarucki

Institut für Hochenergiephysik, Wien, Austria

V. Chekhovsky, A. Litomin, V. Makarenko, J. Suarez Gonzalez

Institute for Nuclear Problems, Minsk, Belarus

M.R. Darwish², E.A. De Wolf, D. Di Croce, X. Janssen, T. Kello³, A. Lelek, M. Pieters, H. Rejeb Sfar, H. Van Haevermaet, P. Van Mechelen, S. Van Putte, N. Van Remortel

Universiteit Antwerpen, Antwerpen, Belgium

F. Blekman, E.S. Bols, S.S. Chhibra, J. D'Hondt, J. De Clercq, D. Lontkovskiy, S. Lowette, I. Marchesini, S. Moortgat, A. Morton, Q. Python, S. Tavernier, W. Van Doninck, P. Van Mulders

Vrije Universiteit Brussel, Brussel, Belgium

D. Beghin, B. Bilin, B. Clerbaux, G. De Lentdecker, B. Dorney, L. Favart, A. Grebenyuk, A.K. Kalsi, I. Makarenko, L. Moureaux, L. Pétré, A. Popov, N. Postiau, E. Starling, L. Thomas, C. Vander Velde, P. Vanlaer, D. Vannerom, L. Wezenbeek

Université Libre de Bruxelles, Bruxelles, Belgium

T. Cornelis, D. Dobur, M. Gruchala, I. Khvastunov⁴, M. Niedziela, C. Roskas, K. Skovpen, M. Tytgat, W. Verbeke, B. Vermassen, M. Vit

Ghent University, Ghent, Belgium

G. Bruno, F. Bury, C. Caputo, P. David, C. Delaere, M. Delcourt, I.S. Donertas, A. Giammanco, V. Lemaitre, K. Mondal, J. Prisciandaro, A. Taliencio, M. Teklishyn, P. Vischia, S. Wertz, S. Wuyckens

Université Catholique de Louvain, Louvain-la-Neuve, Belgium

G.A. Alves, C. Hensel, A. Moraes

Centro Brasileiro de Pesquisas Físicas, Rio de Janeiro, Brazil

W.L. Aldá Júnior, E. Belchior Batista Das Chagas, H. Brandao Malbouisson, W. Carvalho, J. Chinellato⁵, E. Coelho, E.M. Da Costa, G.G. Da Silveira⁶, D. De Jesus Damiao, S. Fonseca De Souza, J. Martins⁷, D. Matos Figueiredo, M. Medina Jaime⁸, C. Mora Herrera, L. Mundim, H. Nogima, P. Rebello Teles, L.J. Sanchez Rosas, A. Santoro, S.M. Silva Do Amaral, A. Sznajder, M. Thiel, F. Torres Da Silva De Araujo, A. Vilela Pereira

Universidade do Estado do Rio de Janeiro, Rio de Janeiro, Brazil

C.A. Bernardes^a, L. Calligaris^a, T.R. Fernandez Perez Tomei^a, E.M. Gregores^{a,b}, D.S. Lemos^a, P.G. Mercadante^{a,b}, S.F. Novaes^a, Sandra S. Padula^a

^a *Universidade Estadual Paulista, São Paulo, Brazil*

^b *Universidade Federal do ABC, São Paulo, Brazil*

A. Aleksandrov, G. Antchev, I. Atanasov, R. Hadjiiska, P. Iaydjiev, M. Misheva, M. Rodozov, M. Shopova, G. Sultanov

Institute for Nuclear Research and Nuclear Energy, Bulgarian Academy of Sciences, Sofia, Bulgaria

A. Dimitrov, T. Ivanov, L. Litov, B. Pavlov, P. Petkov, A. Petrov

University of Sofia, Sofia, Bulgaria

T. Cheng, W. Fang³, Q. Guo, H. Wang, L. Yuan

Beihang University, Beijing, China

M. Ahmad, G. Bauer, Z. Hu, Y. Wang, K. Yi^{9,10}

Department of Physics, Tsinghua University, Beijing, China

E. Chapon, G.M. Chen¹¹, H.S. Chen¹¹, M. Chen, T. Javaid¹¹, A. Kapoor, D. Leggat, H. Liao, Z.-A. Liu¹¹, R. Sharma, A. Spiezia, J. Tao, J. Thomas-wilsker, J. Wang, H. Zhang, S. Zhang¹¹, J. Zhao

Institute of High Energy Physics, Beijing, China

A. Agapitos, Y. Ban, C. Chen, Q. Huang, A. Levin, Q. Li, M. Lu, X. Lyu, Y. Mao, S.J. Qian, D. Wang, Q. Wang, J. Xiao

State Key Laboratory of Nuclear Physics and Technology, Peking University, Beijing, China

Z. You

Sun Yat-Sen University, Guangzhou, China

X. Gao³

Institute of Modern Physics and Key Laboratory of Nuclear Physics and Ion-beam Application (MOE) – Fudan University, Shanghai, China

M. Xiao

Zhejiang University, Hangzhou, China

C. Avila, A. Cabrera, C. Florez, J. Fraga, A. Sarkar, M.A. Segura Delgado

Universidad de Los Andes, Bogota, Colombia

J. Jaramillo, J. Mejia Guisao, F. Ramirez, J.D. Ruiz Alvarez, C.A. Salazar González, N. Vanegas Arbelaez

Universidad de Antioquia, Medellin, Colombia

D. Giljanovic, N. Godinovic, D. Lelas, I. Puljak

University of Split, Faculty of Electrical Engineering, Mechanical Engineering and Naval Architecture, Split, Croatia

Z. Antunovic, M. Kovac, T. Sculac

University of Split, Faculty of Science, Split, Croatia

V. Brigljevic, D. Ferencek, D. Majumder, M. Roguljic, A. Starodumov¹², T. Susa

Institute Rudjer Boskovic, Zagreb, Croatia

M.W. Ather, A. Attikis, E. Erodotou, A. Ioannou, G. Kole, M. Kolosova, S. Konstantinou, J. Mousa, C. Nicolaou, F. Ptochos, P.A. Razis, H. Rykaczewski, H. Saka, D. Tsiakkouri

University of Cyprus, Nicosia, Cyprus

M. Finger¹³, M. Finger Jr.¹³, A. Kveton, J. Tomsa

Charles University, Prague, Czech Republic

E. Ayala

Escuela Politecnica Nacional, Quito, Ecuador

E. Carrera Jarrin

Universidad San Francisco de Quito, Quito, Ecuador

S. Abu Zeid¹⁴, S. Khalil¹⁵, E. Salama^{16,14}

Academy of Scientific Research and Technology of the Arab Republic of Egypt, Egyptian Network of High Energy Physics, Cairo, Egypt

M.A. Mahmoud, Y. Mohammed¹⁷

Center for High Energy Physics (CHEP-FU), Fayoum University, El-Fayoum, Egypt

S. Bhowmik, A. Carvalho Antunes De Oliveira, R.K. Dewanjee, K. Ehataht, M. Kadastik, M. Raidal, C. Veelken

National Institute of Chemical Physics and Biophysics, Tallinn, Estonia

P. Eerola, L. Forthomme, H. Kirschenmann, K. Osterberg, M. Voutilainen

Department of Physics, University of Helsinki, Helsinki, Finland

E. Brücken, F. Garcia, J. Havukainen, V. Karimäki, M.S. Kim, R. Kinnunen, T. Lampén, K. Lassila-Perini, S. Lehti, T. Lindén, H. Siikonen, E. Tuominen, J. Tuominiemi

Helsinki Institute of Physics, Helsinki, Finland

P. Luukka, T. Tuuva

Lappeenranta University of Technology, Lappeenranta, Finland

C. Amendola, M. Besancon, F. Couderc, M. Dejardin, D. Denegri, J.L. Faure, F. Ferri, S. Ganjour, A. Givernaud, P. Gras, G. Hamel de Monchenault, P. Jarry, B. Lenzi, E. Locci, J. Malcles, J. Rander, A. Rosowsky, M.Ö. Sahin, A. Savoy-Navarro¹⁸, M. Titov, G.B. Yu

IRFU, CEA, Université Paris-Saclay, Gif-sur-Yvette, France

S. Ahuja, F. Beaudette, M. Bonanomi, A. Buchot Perraguin, P. Busson, C. Charlot, O. Davignon, B. Diab, G. Falmagne, R. Granier de Cassagnac, A. Hakimi, I. Kucher, A. Lobanov, C. Martin Perez, M. Nguyen, C. Ochando, P. Paganini, J. Rembser, R. Salerno, J.B. Sauvan, Y. Sirois, A. Zabi, A. Zghiche

Laboratoire Leprince-Ringuet, CNRS/IN2P3, Ecole Polytechnique, Institut Polytechnique de Paris, Palaiseau, France

J.-L. Agram¹⁹, J. Andrea, D. Bloch, G. Bourgatte, J.-M. Brom, E.C. Chabert, C. Collard, J.-C. Fontaine¹⁹, D. Gelé, U. Goerlach, C. Grimault, A.-C. Le Bihan, P. Van Hove

Université de Strasbourg, CNRS, IPHC UMR 7178, Strasbourg, France

E. Asilar, S. Beauceron, C. Bernet, G. Boudoul, C. Camen, A. Carle, N. Chanon, D. Contardo, P. Depasse, H. El Mamouni, J. Fay, S. Gascon, M. Gouzevitch, B. Ille, Sa. Jain, I.B. Laktineh, H. Lattaud, A. Lesauvage, M. Lethuillier, L. Mirabito, L. Torterotot, G. Touquet, M. Vander Donckt, S. Viret

Université de Lyon, Université Claude Bernard Lyon 1, CNRS-IN2P3, Institut de Physique Nucléaire de Lyon, Villeurbanne, France

I. Bagaturia²⁰, Z. Tsamalaidze¹³

Georgian Technical University, Tbilisi, Georgia

L. Feld, K. Klein, M. Lipinski, D. Meuser, A. Pauls, M. Preuten, M.P. Rauch, J. Schulz, M. Teroerde

RWTH Aachen University, I. Physikalisches Institut, Aachen, Germany

D. Eliseev, M. Erdmann, P. Fackeldey, B. Fischer, S. Ghosh, T. Hebbeker, K. Hoepfner, H. Keller, L. Mastrolorenzo, M. Merschmeyer, A. Meyer, G. Mocellin, S. Mondal, S. Mukherjee, D. Noll, A. Novak, T. Pook, A. Pozdnyakov, Y. Rath, H. Reithler, J. Roemer, A. Schmidt, S.C. Schuler, A. Sharma, S. Wiedenbeck, S. Zaleski

RWTH Aachen University, III. Physikalisches Institut A, Aachen, Germany

C. Dziwok, G. Flügge, W. Haj Ahmad²¹, O. Hlushchenko, T. Kress, A. Nowack, C. Pistone, O. Pooth, D. Roy, H. Sert, A. Stahl²², T. Ziemons

RWTH Aachen University, III. Physikalisches Institut B, Aachen, Germany

H. Aarup Petersen, M. Aldaya Martin, P. Asmuss, I. Babounikau, S. Baxter, O. Behnke, A. Bermúdez Martínez, A.A. Bin Anuar, K. Borras²³, V. Botta, D. Brunner, A. Campbell, A. Cardini, P. Connor, S. Consuegra Rodríguez, V. Danilov, A. De Wit, M.M. Defranchis, L. Didikh, D. Domínguez Damiani, G. Eckerlin, D. Eckstein, T. Eichhorn, L.I. Estevez Banos, E. Gallo²⁴, A. Geiser, A. Giraldi, A. Grohsjean, M. Guthoff, A. Harb, A. Jafari²⁵, N.Z. Jomhari, H. Jung, A. Kasem²³, M. Kasemann, H. Kaveh, C. Kleinwort, J. Knolle, D. Krücker, W. Lange, T. Lenz, J. Lidrych, K. Lipka, W. Lohmann²⁶, T. Madlener, R. Mankel, I.-A. Melzer-Pellmann, J. Metwally, A.B. Meyer, M. Meyer, M. Missiroli, J. Mnich, A. Mussgiller, V. Myronenko, Y. Otariid, D. Pérez Adán, S.K. Pflitsch, D. Pitzl, A. Raspereza, A. Saggio, A. Saibel, M. Savitskyi, V. Scheurer, C. Schwanenberger, A. Singh, R.E. Sosa Ricardo, N. Tonon, O. Turkot, A. Vagnerini, M. Van De Klundert, R. Walsh, D. Walter, Y. Wen, K. Wichmann, C. Wissing, S. Wuchterl, O. Zenaiev, R. Zlebcik

Deutsches Elektronen-Synchrotron, Hamburg, Germany

R. Aggleton, S. Bein, L. Benato, A. Benecke, K. De Leo, T. Dreyer, A. Ebrahimi, M. Eich, F. Feindt, A. Fröhlich, C. Garbers, E. Garutti, P. Gunnellini, J. Haller, A. Hinzmann, A. Karavdina, G. Kasieczka, R. Klanner, R. Kogler, V. Kutzner, J. Lange, T. Lange, A. Malara, C.E.N. Niemeyer, A. Nigamova, K.J. Pena Rodriguez, O. Rieger, P. Schleper, S. Schumann, J. Schwandt, D. Schwarz, J. Sonneveld, H. Stadie, G. Steinbrück, B. Vormwald, I. Zoi

University of Hamburg, Hamburg, Germany

J. Bechtel, T. Berger, E. Butz, R. Caspart, T. Chwalek, W. De Boer, A. Dierlamm, A. Droll, K. El Morabit, N. Faltermann, K. Flöh, M. Giffels, A. Gottmann, F. Hartmann²², C. Heidecker, U. Husemann, I. Katkov²⁷, P. Keicher, R. Koppenhöfer, S. Maier, M. Metzler, S. Mitra, D. Müller, Th. Müller, M. Musich, G. Quast, K. Rabbertz, J. Rauser, D. Savoii, D. Schäfer, M. Schnepf, M. Schröder, D. Seith, I. Shvetsov, H.J. Simonis, R. Ulrich, M. Wassmer, M. Weber, R. Wolf, S. Wozniewski

Karlsruher Institut fuer Technologie, Karlsruhe, Germany

G. Anagnostou, P. Asenov, G. Daskalakis, T. Geralis, A. Kyriakis, D. Loukas, G. Paspalaki, A. Stakia

Institute of Nuclear and Particle Physics (INPP), NCSR Demokritos, Aghia Paraskevi, Greece

M. Diamantopoulou, D. Karasavvas, G. Karathanasis, P. Kontaxakis, C.K. Koraka, A. Manousakis-katsikakis, A. Panagiotou, I. Papavergou, N. Saoulidou, K. Theofilatos, K. Vellidis, E. Vourliotis

National and Kapodistrian University of Athens, Athens, Greece

G. Bakas, K. Kousouris, I. Papakrivopoulos, G. Tsipolitis, A. Zacharopoulou

National Technical University of Athens, Athens, Greece

I. Evangelou, C. Foudas, P. Gianneios, P. Katsoulis, P. Kokkas, K. Manitaras, N. Manthos, I. Papadopoulos, J. Strologas

University of Ioánnina, Ioánnina, Greece

M. Bartók²⁸, M. Csanad, M.M.A. Gadallah²⁹, S. Lökös³⁰, P. Major, K. Mandal, A. Mehta, G. Pasztor, O. Surányi, G.I. Veres

MTA-ELTE Lendület CMS Particle and Nuclear Physics Group, Eötvös Loránd University, Budapest, Hungary

G. Bencze, C. Hajdu, D. Horvath³¹, F. Sikler, V. Veszpremi, G. Vesztergombi[†]

Wigner Research Centre for Physics, Budapest, Hungary

S. Czellar, J. Karancsi²⁸, J. Molnar, Z. Szillasi, D. Teyssier

Institute of Nuclear Research ATOMKI, Debrecen, Hungary

P. Raics, Z.L. Trocsanyi, B. Ujvari

Institute of Physics, University of Debrecen, Debrecen, Hungary

T. Csorgo³², F. Nemes³², T. Novak

Eszterhazy Karoly University, Karoly Robert Campus, Gyogyos, Hungary

S. Choudhury, J.R. Komaragiri, D. Kumar, L. Panwar, P.C. Tiwari

Indian Institute of Science (IISc), Bangalore, India

S. Bahinipati³³, D. Dash, C. Kar, P. Mal, T. Mishra, V.K. Muraleedharan Nair Bindhu, A. Nayak³⁴,
D.K. Sahoo³³, N. Sur, S.K. Swain

National Institute of Science Education and Research, HBNI, Bhubaneswar, India

S. Bansal, S.B. Beri, V. Bhatnagar, G. Chaudhary, S. Chauhan, N. Dhingra³⁵, R. Gupta, A. Kaur, S. Kaur,
P. Kumari, M. Meena, K. Sandeep, S. Sharma, J.B. Singh, A.K. Viridi

Panjab University, Chandigarh, India

A. Ahmed, A. Bhardwaj, B.C. Choudhary, R.B. Garg, M. Gola, S. Keshri, A. Kumar, M. Naimuddin,
P. Priyanka, K. Ranjan, A. Shah

University of Delhi, Delhi, India

M. Bharti³⁶, R. Bhattacharya, S. Bhattacharya, D. Bhowmik, S. Dutta, S. Ghosh, B. Gomber³⁷, M. Maity³⁸,
S. Nandan, P. Palit, P.K. Rout, G. Saha, B. Sahu, S. Sarkar, M. Sharan, B. Singh³⁶, S. Thakur³⁶

Saha Institute of Nuclear Physics, HBNI, Kolkata, India

P.K. Behera, S.C. Behera, P. Kalbhor, A. Muhammad, R. Pradhan, P.R. Pujahari, A. Sharma, A.K. Sikdar

Indian Institute of Technology Madras, Madras, India

D. Dutta, V. Kumar, K. Naskar³⁹, P.K. Netrakanti, L.M. Pant, P. Shukla

Bhabha Atomic Research Centre, Mumbai, India

T. Aziz, M.A. Bhat, S. Dugad, R. Kumar Verma, G.B. Mohanty, U. Sarkar

Tata Institute of Fundamental Research-A, Mumbai, India

S. Banerjee, S. Bhattacharya, S. Chatterjee, R. Chudasama, M. Guchait, S. Karmakar, S. Kumar,
G. Majumder, K. Mazumdar, S. Mukherjee, D. Roy

Tata Institute of Fundamental Research-B, Mumbai, India

S. Dube, B. Kansal, S. Pandey, A. Rane, A. Rastogi, S. Sharma

Indian Institute of Science Education and Research (IISER), Pune, India

H. Bakhshiansohi⁴⁰, M. Zeinali⁴¹

Department of Physics, Isfahan University of Technology, Isfahan, Iran

S. Chenarani⁴², S.M. Etesami, M. Khakzad, M. Mohammadi Najafabadi

Institute for Research in Fundamental Sciences (IPM), Tehran, Iran

M. Felcini, M. Grunewald

University College Dublin, Dublin, Ireland

M. Abbrescia^{a,b}, R. Aly^{a,b,43}, C. Aruta^{a,b}, A. Colaleo^a, D. Creanza^{a,c}, N. De Filippis^{a,c}, M. De Palma^{a,b},
A. Di Florio^{a,b}, A. Di Pilato^{a,b}, W. Elmetenawee^{a,b}, L. Fiore^a, A. Gelmi^{a,b}, M. Gul^a, G. Iaselli^{a,c},
M. Ince^{a,b}, S. Lezki^{a,b}, G. Maggi^{a,c}, M. Maggi^a, I. Margjeka^{a,b}, V. Mastrapasqua^{a,b}, J.A. Merlin^a,

S. My^{a,b}, S. Nuzzo^{a,b}, A. Pompili^{a,b}, G. Pugliese^{a,c}, A. Ranieri^a, G. Selvaggi^{a,b}, L. Silvestris^a,
F.M. Simone^{a,b}, R. Venditti^a, P. Verwilligen^a

^a INFN Sezione di Bari, Bari, Italy

^b Università di Bari, Bari, Italy

^c Politecnico di Bari, Bari, Italy

G. Abbiendi^a, C. Battilana^{a,b}, D. Bonacorsi^{a,b}, L. Borgonovi^a, S. Braibant-Giacomelli^{a,b}, R. Campanini^{a,b},
P. Capiluppi^{a,b}, A. Castro^{a,b}, F.R. Cavallo^a, C. Ciocca^a, M. Cuffiani^{a,b}, G.M. Dallavalle^a, T. Diotallevi^{a,b},
F. Fabbri^a, A. Fanfani^{a,b}, E. Fontanesi^{a,b}, P. Giacomelli^a, L. Giommi^{a,b}, C. Grandi^a, L. Guiducci^{a,b},
F. Iemmi^{a,b}, S. Lo Meo^{a,44}, S. Marcellini^a, G. Masetti^a, F.L. Navarra^{a,b}, A. Perrotta^a, F. Primavera^{a,b},
A.M. Rossi^{a,b}, T. Rovelli^{a,b}, G.P. Siroli^{a,b}, N. Tosi^a

^a INFN Sezione di Bologna, Bologna, Italy

^b Università di Bologna, Bologna, Italy

S. Albergo^{a,b,45}, S. Costa^{a,b}, A. Di Mattia^a, R. Potenza^{a,b}, A. Tricomi^{a,b,45}, C. Tuve^{a,b}

^a INFN Sezione di Catania, Catania, Italy

^b Università di Catania, Catania, Italy

G. Barbagli^a, A. Cassese^a, R. Ceccarelli^{a,b}, V. Ciulli^{a,b}, C. Civinini^a, R. D'Alessandro^{a,b}, F. Fiori^a,
E. Focardi^{a,b}, G. Latino^{a,b}, P. Lenzi^{a,b}, M. Lizzo^{a,b}, M. Meschini^a, S. Paoletti^a, R. Seidita^{a,b},
G. Sguazzoni^a, L. Viliani^a

^a INFN Sezione di Firenze, Firenze, Italy

^b Università di Firenze, Firenze, Italy

L. Benussi, S. Bianco, D. Piccolo

INFN Laboratori Nazionali di Frascati, Frascati, Italy

M. Bozzo^{a,b}, F. Ferro^a, R. Mulargia^{a,b}, E. Robutti^a, S. Tosi^{a,b}

^a INFN Sezione di Genova, Genova, Italy

^b Università di Genova, Genova, Italy

A. Benaglia^a, A. Beschi^{a,b}, F. Brivio^{a,b}, F. Ceteorelli^{a,b}, V. Ciriolo^{a,b,22}, F. De Guio^{a,b}, M.E. Dinardo^{a,b},
P. Dini^a, S. Gennai^a, A. Ghezzi^{a,b}, P. Govoni^{a,b}, L. Guzzi^{a,b}, M. Malberti^a, S. Malvezzi^a, A. Massironi^a,
D. Menasce^a, F. Monti^{a,b}, L. Moroni^a, M. Paganoni^{a,b}, D. Pedrini^a, S. Ragazzi^{a,b}, T. Tabarelli de Fatis^{a,b},
D. Valsecchi^{a,b,22}, D. Zuolo^{a,b}

^a INFN Sezione di Milano-Bicocca, Milano, Italy

^b Università di Milano-Bicocca, Milano, Italy

S. Buontempo^a, N. Cavallo^{a,c}, A. De Iorio^{a,b}, F. Fabozzi^{a,c}, F. Fienga^a, A.O.M. Iorio^{a,b}, L. Lista^{a,b},
S. Meola^{a,d,22}, P. Paolucci^{a,22}, B. Rossi^a, C. Sciacca^{a,b}, E. Voevodina^{a,b}

^a INFN Sezione di Napoli, Napoli, Italy

^b Università di Napoli 'Federico II', Napoli, Italy

^c Università della Basilicata, Potenza, Italy

^d Università G. Marconi, Roma, Italy

P. Azzi^a, N. Bacchetta^a, D. Bisello^{a,b}, P. Bortignon^a, A. Bragagnolo^{a,b}, R. Carlin^{a,b}, P. Checchia^a,
P. De Castro Manzano^a, T. Dorigo^a, F. Gasparini^{a,b}, U. Gasparini^{a,b}, S.Y. Hoh^{a,b}, L. Layer^{a,46},
M. Margoni^{a,b}, A.T. Meneguzzo^{a,b}, M. Presilla^{a,b}, P. Ronchese^{a,b}, R. Rossin^{a,b}, F. Simonetto^{a,b},
G. Strong^a, M. Tosi^{a,b}, H. Yarar^{a,b}, M. Zanetti^{a,b}, P. Zotto^{a,b}, A. Zucchetta^{a,b}, G. Zumerle^{a,b}

^a INFN Sezione di Padova, Padova, Italy

^b Università di Padova, Padova, Italy

^c Università di Trento, Trento, Italy

C. Aimè^{a,b}, A. Braghieri^a, S. Calzaferri^{a,b}, D. Fiorina^{a,b}, P. Montagna^{a,b}, S.P. Ratti^{a,b}, V. Re^a,
M. Ressegotti^{a,b}, C. Riccardi^{a,b}, P. Salvini^a, I. Vai^a, P. Vitulo^{a,b}

^a INFN Sezione di Pavia, Pavia, Italy

^b Università di Pavia, Pavia, Italy

M. Biasini ^{a,b}, G.M. Bilei ^a, D. Ciangottini ^{a,b}, L. Fanò ^{a,b}, P. Lariccia ^{a,b}, G. Mantovani ^{a,b}, V. Mariani ^{a,b}, M. Menichelli ^a, F. Moscatelli ^a, A. Piccinelli ^{a,b}, A. Rossi ^{a,b}, A. Santocchia ^{a,b}, D. Spiga ^a, T. Tedeschi ^{a,b}

^a INFN Sezione di Perugia, Perugia, Italy

^b Università di Perugia, Perugia, Italy

K. Androsov ^a, P. Azzurri ^a, G. Bagliesi ^a, V. Bertacchi ^{a,c}, L. Bianchini ^a, T. Boccali ^a, R. Castaldi ^a, M.A. Ciocci ^{a,b}, R. Dell'Orso ^a, M.R. Di Domenico ^{a,b}, S. Donato ^a, L. Giannini ^{a,c}, A. Giassi ^a, M.T. Grippo ^a, F. Ligabue ^{a,c}, E. Manca ^{a,c}, G. Mandorli ^{a,c}, A. Messineo ^{a,b}, F. Palla ^a, G. Ramirez-Sanchez ^{a,c}, A. Rizzi ^{a,b}, G. Rolandi ^{a,c}, S. Roy Chowdhury ^{a,c}, A. Scribano ^a, N. Shafiei ^{a,b}, P. Spagnolo ^a, R. Tenchini ^a, G. Tonelli ^{a,b}, N. Turini ^a, A. Venturi ^a, P.G. Verdini ^a

^a INFN Sezione di Pisa, Pisa, Italy

^b Università di Pisa, Pisa, Italy

^c Scuola Normale Superiore di Pisa, Pisa, Italy

F. Cavallari ^a, M. Cipriani ^{a,b}, D. Del Re ^{a,b}, E. Di Marco ^a, M. Diemoz ^a, E. Longo ^{a,b}, P. Meridiani ^a, G. Organtini ^{a,b}, F. Pandolfi ^a, R. Paramatti ^{a,b}, C. Quaranta ^{a,b}, S. Rahatlou ^{a,b}, C. Rovelli ^a, F. Santanastasio ^{a,b}, L. Soffi ^{a,b}, R. Tramontano ^{a,b}

^a INFN Sezione di Roma, Rome, Italy

^b Sapienza Università di Roma, Rome, Italy

N. Amapane ^{a,b}, R. Arcidiacono ^{a,c}, S. Argiro ^{a,b}, M. Arneodo ^{a,c}, N. Bartosik ^a, R. Bellan ^{a,b}, A. Bellora ^{a,b}, J. Berenguer Antequera ^{a,b}, C. Biino ^a, A. Cappati ^{a,b}, N. Cartiglia ^a, S. Cometti ^a, M. Costa ^{a,b}, R. Covarelli ^{a,b}, N. Demaria ^a, B. Kiani ^{a,b}, F. Legger ^a, C. Mariotti ^a, S. Maselli ^a, E. Migliore ^{a,b}, V. Monaco ^{a,b}, E. Monteil ^{a,b}, M. Monteno ^a, M.M. Obertino ^{a,b}, G. Ortona ^a, L. Pacher ^{a,b}, N. Pastrone ^a, M. Pelliccioni ^a, G.L. Pinna Angioni ^{a,b}, M. Ruspa ^{a,c}, R. Salvatico ^{a,b}, F. Siviero ^{a,b}, V. Sola ^a, A. Solano ^{a,b}, D. Soldi ^{a,b}, A. Staiano ^a, M. Tornago ^{a,b}, D. Trocino ^{a,b}

^a INFN Sezione di Torino, Torino, Italy

^b Università di Torino, Torino, Italy

^c Università del Piemonte Orientale, Novara, Italy

S. Belforte ^a, V. Candelise ^{a,b}, M. Casarsa ^a, F. Cossutti ^a, A. Da Rold ^{a,b}, G. Della Ricca ^{a,b}, F. Vazzoler ^{a,b}

^a INFN Sezione di Trieste, Trieste, Italy

^b Università di Trieste, Trieste, Italy

S. Dogra, C. Huh, B. Kim, D.H. Kim, G.N. Kim, J. Lee, S.W. Lee, C.S. Moon, Y.D. Oh, S.I. Pak, B.C. Radburn-Smith, S. Sekmen, Y.C. Yang

Kyungpook National University, Daegu, Republic of Korea

H. Kim, D.H. Moon

Chonnam National University, Institute for Universe and Elementary Particles, Kwangju, Republic of Korea

B. Francois, T.J. Kim, J. Park

Hanyang University, Seoul, Republic of Korea

S. Cho, S. Choi, Y. Go, S. Ha, B. Hong, K. Lee, K.S. Lee, J. Lim, J. Park, S.K. Park, J. Yoo

Korea University, Seoul, Republic of Korea

J. Goh, A. Gurtu

Kyung Hee University, Department of Physics, Seoul, Republic of Korea

H.S. Kim, Y. Kim

Sejong University, Seoul, Republic of Korea

J. Almond, J.H. Bhyun, J. Choi, S. Jeon, J. Kim, J.S. Kim, S. Ko, H. Kwon, H. Lee, K. Lee, S. Lee, K. Nam, B.H. Oh, M. Oh, S.B. Oh, H. Seo, U.K. Yang, I. Yoon

Seoul National University, Seoul, Republic of Korea

D. Jeon, J.H. Kim, B. Ko, J.S.H. Lee, I.C. Park, Y. Roh, D. Song, I.J. Watson

University of Seoul, Seoul, Republic of Korea

H.D. Yoo

Yonsei University, Department of Physics, Seoul, Republic of Korea

Y. Choi, C. Hwang, Y. Jeong, H. Lee, Y. Lee, I. Yu

Sungkyunkwan University, Suwon, Republic of Korea

Y. Maghrbi

College of Engineering and Technology, American University of the Middle East (AUM), Kuwait

V. Veckalns⁴⁷

Riga Technical University, Riga, Latvia

A. Juodagalvis, A. Rinkevicius, G. Tamulaitis, A. Vaitkevicius

Vilnius University, Vilnius, Lithuania

W.A.T. Wan Abdullah, M.N. Yusli, Z. Zolkapli

National Centre for Particle Physics, Universiti Malaya, Kuala Lumpur, Malaysia

J.F. Benitez, A. Castaneda Hernandez, J.A. Murillo Quijada, L. Valencia Palomo

Universidad de Sonora (UNISON), Hermosillo, Mexico

G. Ayala, H. Castilla-Valdez, E. De La Cruz-Burelo, I. Heredia-De La Cruz⁴⁸, R. Lopez-Fernandez, C.A. Mondragon Herrera, D.A. Perez Navarro, A. Sanchez-Hernandez

Centro de Investigacion y de Estudios Avanzados del IPN, Mexico City, Mexico

S. Carrillo Moreno, C. Oropeza Barrera, M. Ramirez-Garcia, F. Vazquez Valencia

Universidad Iberoamericana, Mexico City, Mexico

J. Eysermans, I. Pedraza, H.A. Salazar Ibarquen, C. Uribe Estrada

Benemerita Universidad Autonoma de Puebla, Puebla, Mexico

A. Morelos Pineda

Universidad Autónoma de San Luis Potosí, San Luis Potosí, Mexico

J. Mijuskovic⁴, N. Raicevic

University of Montenegro, Podgorica, Montenegro

D. Krofcheck

University of Auckland, Auckland, New Zealand

S. Bheesette, P.H. Butler

University of Canterbury, Christchurch, New Zealand

A. Ahmad, M.I. Asghar, A. Awais, M.I.M. Awan, H.R. Hoorani, W.A. Khan, M.A. Shah, M. Shoaib, M. Waqas

National Centre for Physics, Quaid-I-Azam University, Islamabad, Pakistan

V. Avati, L. Grzanka, M. Malawski

AGH University of Science and Technology Faculty of Computer Science, Electronics and Telecommunications, Krakow, Poland

H. Bialkowska, M. Bluj, B. Boimska, T. Frueboes, M. Górski, M. Kazana, M. Szeleper, P. Traczyk, P. Zalewski

National Centre for Nuclear Research, Swierk, Poland

K. Bunkowski, K. Doroba, A. Kalinowski, M. Konecki, J. Krolikowski, M. Walczak

Institute of Experimental Physics, Faculty of Physics, University of Warsaw, Warsaw, Poland

M. Araujo, P. Bargassa, D. Bastos, A. Boletti, P. Faccioli, M. Gallinaro, J. Hollar, N. Leonardo, T. Niknejad, J. Seixas, K. Shchelina, O. Toldaiev, J. Varela

Laboratório de Instrumentação e Física Experimental de Partículas, Lisboa, Portugal

S. Afanasiev, A. Baginyan, P. Bunin, Y. Ershov, M. Gavrilenko, A. Golunov, I. Golutvin, I. Gorbunov, A. Kamenev, V. Karjavine, I. Kashunin, A. Lanev, A. Malakhov, V. Matveev^{49,50}, V. Palichik, V. Perelygin, M. Savina, S. Shmatov, V. Smirnov, O. Teryaev, B.S. Yuldashev⁵¹, A. Zarubin

Joint Institute for Nuclear Research, Dubna, Russia

G. Gavrilo, V. Golovtsov, Y. Ivanov, V. Kim⁵², E. Kuznetsova⁵³, V. Murzin, V. Oreshkin, I. Smirnov, D. Sosnov, V. Sulimov, L. Uvarov, S. Volkov, A. Vorobyev

Petersburg Nuclear Physics Institute, Gatchina (St. Petersburg), Russia

Yu. Andreev, A. Dermenev, S. Gninenko, N. Golubev, A. Karneyeu, M. Kirsanov, N. Krasnikov, A. Pashenkov, G. Pivovarov, D. Tlisov[†], A. Toropin

Institute for Nuclear Research, Moscow, Russia

V. Epshteyn, V. Gavrilo, N. Lychkovskaya, A. Nikitenko⁵⁴, V. Popov, G. Safronov, A. Spiridonov, A. Stepenov, M. Toms, E. Vlasov, A. Zhokin

Institute for Theoretical and Experimental Physics named by A.I. Alikhanov of NRC 'Kurchatov Institute', Moscow, Russia

T. Aushev

Moscow Institute of Physics and Technology, Moscow, Russia

R. Chistov⁵⁵, M. Danilov⁵⁶, A. Oskin, P. Parygin, S. Polikarpov⁵⁵

National Research Nuclear University 'Moscow Engineering Physics Institute' (MEPhI), Moscow, Russia

V. Andreev, M. Azarkin, I. Dremin, M. Kirakosyan, A. Terkulov

P.N. Lebedev Physical Institute, Moscow, Russia

A. Belyaev, E. Boos, V. Bunichev, M. Dubinin⁵⁷, L. Dudko, A. Ershov, A. Gribushin, V. Klyukhin, O. Kodolova, I. Lokhtin, S. Obraztsov, V. Savrin, A. Snigirev

Skobeltsyn Institute of Nuclear Physics, Lomonosov Moscow State University, Moscow, Russia

V. Blinov⁵⁸, T. Dimova⁵⁸, L. Kardapoltsev⁵⁸, I. Ovtin⁵⁸, Y. Skovpen⁵⁸

Novosibirsk State University (NSU), Novosibirsk, Russia

I. Azhgirey, I. Bayshev, V. Kachanov, A. Kalinin, D. Konstantinov, V. Petrov, R. Ryutin, A. Sobol, S. Troshin, N. Tyurin, A. Uzunian, A. Volkov

Institute for High Energy Physics of National Research Centre 'Kurchatov Institute', Protvino, Russia

A. Babaev, A. Iuzhakov, V. Okhotnikov, L. Sukhikh

National Research Tomsk Polytechnic University, Tomsk, Russia

V. Borchsh, V. Ivanchenko, E. Tcherniaev

Tomsk State University, Tomsk, Russia

P. Adzic⁵⁹, P. Cirkovic, M. Dordevic, P. Milenovic, J. Milosevic

University of Belgrade: Faculty of Physics and VINCA Institute of Nuclear Sciences, Belgrade, Serbia

M. Aguilar-Benitez, J. Alcaraz Maestre, A. Álvarez Fernández, I. Bachiller, M. Barrio Luna, Cristina F. Bedoya, C.A. Carrillo Montoya, M. Cepeda, M. Cerrada, N. Colino, B. De La Cruz, A. Delgado Peris, J.P. Fernández Ramos, J. Flix, M.C. Fouz, A. García Alonso, O. Gonzalez Lopez, S. Goy Lopez, J.M. Hernandez, M.I. Josa, J. León Holgado, D. Moran, Á. Navarro Tobar, A. Pérez-Calero Yzquierdo, J. Puerta Pelayo, I. Redondo, L. Romero, S. Sánchez Navas, M.S. Soares, A. Triossi, L. Urda Gómez, C. Willmott

Centro de Investigaciones Energéticas Medioambientales y Tecnológicas (CIEMAT), Madrid, Spain

C. Albajar, J.F. de Trocóniz, R. Reyes-Almanza

Universidad Autónoma de Madrid, Madrid, Spain

B. Alvarez Gonzalez, J. Cuevas, C. Erice, J. Fernandez Menendez, S. Folgueras, I. Gonzalez Caballero, E. Palencia Cortezon, C. Ramón Álvarez, J. Ripoll Sau, V. Rodríguez Bouza, S. Sanchez Cruz, A. Trapote

Universidad de Oviedo, Instituto Universitario de Ciencias y Tecnologías Espaciales de Asturias (ICTEA), Oviedo, Spain

J.A. Brochero Cifuentes, I.J. Cabrillo, A. Calderon, B. Chazin Quero, J. Duarte Campderros, M. Fernandez, P.J. Fernández Manteca, G. Gomez, C. Martinez Rivero, P. Martinez Ruiz del Arbol, F. Matorras, J. Piedra Gomez, C. Prieels, F. Ricci-Tam, T. Rodrigo, A. Ruiz-Jimeno, L. Scodellaro, I. Vila, J.M. Vizan Garcia

Instituto de Física de Cantabria (IFCA), CSIC-Universidad de Cantabria, Santander, Spain

M.K. Jayananda, B. Kailasapathy⁶⁰, D.U.J. Sonnadara, D.D.C. Wickramarathna

University of Colombo, Colombo, Sri Lanka

W.G.D. Dharmaratna, K. Liyanage, N. Perera, N. Wickramage

University of Ruhuna, Department of Physics, Matara, Sri Lanka

T.K. Aarrestad, D. Abbaneo, B. Akgun, E. Auffray, G. Auzinger, J. Baechler, P. Baillon, A.H. Ball, D. Barney, J. Bendavid, N. Beni, M. Bianco, A. Bocci, E. Bossini, E. Brondolin, T. Camporesi, G. Cerminara, L. Cristella, D. d'Enterria, A. Dabrowski, N. Daci, V. Daponte, A. David, A. De Roeck, M. Deile, R. Di Maria, M. Dobson, M. Dünser, N. Dupont, A. Elliott-Peisert, N. Emrskova, F. Fallavollita⁶¹, D. Fasanella, S. Fiorendi, A. Florent, G. Franzoni, J. Fulcher, W. Funk, S. Giani, D. Gigi, K. Gill, F. Glege, L. Gouskos, M. Guilbaud, D. Gulhan, M. Haranko, J. Hegeman, Y. Iiyama, V. Innocente, T. James, P. Janot, J. Kaspar, J. Kieseler, M. Komm, N. Kratochwil, C. Lange, S. Laurila, P. Lecoq, K. Long, C. Lourenço, L. Malgeri, S. Mallios, M. Mannelli, F. Meijers, S. Mersi, E. Meschi, F. Moortgat, M. Mulders, J. Niedziela, S. Orfanelli, L. Orsini, F. Pantaleo²², L. Pape, E. Perez, M. Peruzzi, A. Petrilli, G. Petrucciani, A. Pfeiffer, M. Pierini, T. Quast, D. Rabad, A. Racz, M. Rieger, M. Rovere, H. Sakulin, J. Salfeld-Nebgen, S. Scarfi, C. Schäfer, C. Schwick, M. Selvaggi, A. Sharma, P. Silva, W. Snoeys, P. Sphicas⁶², S. Summers, V.R. Tavolaro, D. Treille, A. Tsiros, G.P. Van Onsem, A. Vartak, M. Verzetti, K.A. Wozniak, W.D. Zeuner

CERN, European Organization for Nuclear Research, Geneva, Switzerland

L. Caminada⁶³, W. Erdmann, R. Horisberger, Q. Ingram, H.C. Kaestli, D. Kotlinski, U. Langenegger, T. Rohe

Paul Scherrer Institut, Villigen, Switzerland

M. Backhaus, P. Berger, A. Calandri, N. Chernyavskaya, A. De Cosa, G. Dissertori, M. Dittmar, M. Donegà, C. Dorfer, T. Gadek, T.A. Gómez Espinosa, C. Grab, D. Hits, W. Lustermann, A.-M. Lyon, R.A. Manzoni, M.T. Meinhard, F. Micheli, F. Nessi-Tedaldi, F. Pauss, V. Perovic, G. Perrin, S. Pigazzini, M.G. Ratti,

M. Reichmann, C. Reissel, T. Reitenspiess, B. Ristic, D. Ruini, D.A. Sanz Becerra, M. Schönenberger, V. Stampf, J. Steggemann⁶⁴, M.L. Vesterbacka Olsson, R. Wallny, D.H. Zhu

ETH Zurich – Institute for Particle Physics and Astrophysics (IPA), Zurich, Switzerland

C. Amsler⁶⁵, C. Botta, D. Brzhechko, M.F. Canelli, R. Del Burgo, J.K. Heikkilä, M. Huwiler, A. Jofrehei, B. Kilminster, S. Leontsinis, A. Macchiolo, P. Meiring, V.M. Mikuni, U. Molinatti, I. Neutelings, G. Rauco, A. Reimers, P. Robmann, K. Schweiger, Y. Takahashi

Universität Zürich, Zurich, Switzerland

C. Adloff⁶⁶, C.M. Kuo, W. Lin, A. Roy, T. Sarkar³⁸, S.S. Yu

National Central University, Chung-Li, Taiwan

L. Ceard, P. Chang, Y. Chao, K.F. Chen, P.H. Chen, W.-S. Hou, Y.y. Li, R.-S. Lu, E. Paganis, A. Psallidas, A. Steen, E. Yazgan

National Taiwan University (NTU), Taipei, Taiwan

B. Asavapibhop, C. Asawatangtrakuldee, N. Srimanobhas

Chulalongkorn University, Faculty of Science, Department of Physics, Bangkok, Thailand

F. Boran, S. Damarseckin⁶⁷, Z.S. Demiroglu, F. Dolek, C. Dozen⁶⁸, I. Dumanoglu⁶⁹, E. Eskut, G. Gokbulut, Y. Guler, E. Gurpinar Guler⁷⁰, I. Hos⁷¹, C. Isik, E.E. Kangal⁷², O. Kara, A. Kayis Topaksu, U. Kiminsu, G. Onengut, K. Ozdemir⁷³, A. Polatoz, A.E. Simsek, B. Tali⁷⁴, U.G. Tok, S. Turkcapar, I.S. Zorbakir, C. Zorbilmez

Çukurova University, Physics Department, Science and Art Faculty, Adana, Turkey

B. Isildak⁷⁵, G. Karapinar⁷⁶, K. Ocalan⁷⁷, M. Yalvac⁷⁸

Middle East Technical University, Physics Department, Ankara, Turkey

I.O. Atakisi, E. Gülmez, M. Kaya⁷⁹, O. Kaya⁸⁰, Ö. Özçelik, S. Tekten⁸¹, E.A. Yetkin⁸²

Bogazici University, Istanbul, Turkey

A. Cakir, K. Cankocak⁶⁹, Y. Komurcu, S. Sen⁸³

Istanbul Technical University, Istanbul, Turkey

F. Aydogmus Sen, S. Cerci⁷⁴, B. Kaynak, S. Ozkorucuklu, D. Sunar Cerci⁷⁴

Istanbul University, Istanbul, Turkey

B. Grynyov

Institute for Scintillation Materials of National Academy of Science of Ukraine, Kharkov, Ukraine

L. Levchuk

National Scientific Center, Kharkov Institute of Physics and Technology, Kharkov, Ukraine

E. Bhal, S. Bologna, J.J. Brooke, E. Clement, D. Cussans, H. Flacher, J. Goldstein, G.P. Heath, H.F. Heath, L. Kreczko, B. Krikler, S. Paramesvaran, T. Sakuma, S. Seif El Nasr-Storey, V.J. Smith, N. Stylianou⁸⁴, J. Taylor, A. Titterton

University of Bristol, Bristol, United Kingdom

K.W. Bell, A. Belyaev⁸⁵, C. Brew, R.M. Brown, D.J.A. Cockerill, K.V. Ellis, K. Harder, S. Harper, J. Linacre, K. Manolopoulos, D.M. Newbold, E. Olaiya, D. Petyt, T. Reis, T. Schuh, C.H. Shepherd-Themistocleous, A. Thea, I.R. Tomalin, T. Williams

Rutherford Appleton Laboratory, Didcot, United Kingdom

R. Bainbridge, P. Bloch, S. Bonomally, J. Borg, S. Breeze, O. Buchmuller, A. Bundock, V. Cepaitis, G.S. Chahal⁸⁶, D. Colling, P. Dauncey, G. Davies, M. Della Negra, G. Fedi, G. Hall, G. Iles, J. Langford, L. Lyons, A.-M. Magnan, S. Malik, A. Martelli, V. Milosevic, J. Nash⁸⁷, V. Palladino, M. Pesaresi, D.M. Raymond, A. Richards, A. Rose, E. Scott, C. Seez, A. Shtipliyski, M. Stoye, A. Tapper, K. Uchida, T. Virdee²², N. Wardle, S.N. Webb, D. Winterbottom, A.G. Zecchinelli

Imperial College, London, United Kingdom

J.E. Cole, P.R. Hobson, A. Khan, P. Kyberd, C.K. Mackay, I.D. Reid, L. Teodorescu, S. Zahid

Brunel University, Uxbridge, United Kingdom

S. Abdullin, A. Brinkerhoff, K. Call, B. Caraway, J. Dittmann, K. Hatakeyama, A.R. Kanuganti, C. Madrid, B. McMaster, N. Pastika, S. Sawant, C. Smith, J. Wilson

Baylor University, Waco, USA

R. Bartek, A. Dominguez, R. Uniyal, A.M. Vargas Hernandez

Catholic University of America, Washington, DC, USA

A. Buccilli, O. Charaf, S.I. Cooper, S.V. Gleyzer, C. Henderson, C.U. Perez, P. Rumerio, C. West

The University of Alabama, Tuscaloosa, USA

A. Akpinar, A. Albert, D. Arcaro, C. Cosby, Z. Demiragli, D. Gastler, J. Rohlf, K. Salyer, D. Sperka, D. Spitzbart, I. Suarez, S. Yuan, D. Zou

Boston University, Boston, USA

G. Benelli, B. Burkley, X. Coubez²³, D. Cutts, Y.t. Duh, M. Hadley, U. Heintz, J.M. Hogan⁸⁸, K.H.M. Kwok, E. Laird, G. Landsberg, K.T. Lau, J. Lee, M. Narain, S. Sagir⁸⁹, R. Syarif, E. Usai, W.Y. Wong, D. Yu, W. Zhang

Brown University, Providence, USA

R. Band, C. Brainerd, R. Breedon, M. Calderon De La Barca Sanchez, M. Chertok, J. Conway, R. Conway, P.T. Cox, R. Erbacher, C. Flores, G. Funk, F. Jensen, W. Ko[†], O. Kukral, R. Lander, M. Mulhearn, D. Pellett, J. Pilot, M. Shi, D. Taylor, K. Tos, M. Tripathi, Y. Yao, F. Zhang

University of California, Davis, Davis, USA

M. Bachtis, R. Cousins, A. Dasgupta, D. Hamilton, J. Hauser, M. Ignatenko, M.A. Iqbal, T. Lam, N. Mccoll, W.A. Nash, S. Regnard, D. Saltzberg, C. Schnaible, B. Stone, V. Valuev

University of California, Los Angeles, USA

K. Burt, Y. Chen, R. Clare, J.W. Gary, G. Hanson, G. Karapostoli, O.R. Long, N. Manganelli, M. Olmedo Negrete, M.I. Paneva, W. Si, S. Wimpenny, Y. Zhang

University of California, Riverside, Riverside, USA

J.G. Branson, P. Chang, S. Cittolin, S. Cooperstein, N. Deelen, J. Duarte, R. Gerosa, D. Gilbert, V. Krutelyov, J. Letts, M. Masciovecchio, S. May, S. Padhi, M. Pieri, V. Sharma, M. Tadel, F. Würthwein, A. Yagil

University of California, San Diego, La Jolla, USA

N. Amin, C. Campagnari, M. Citron, A. Dorsett, V. Dutta, J. Incandela, B. Marsh, H. Mei, A. Ovcharova, H. Qu, M. Quinnan, J. Richman, U. Sarica, D. Stuart, S. Wang

University of California, Santa Barbara – Department of Physics, Santa Barbara, USA

A. Bornheim, O. Cerri, I. Dutta, J.M. Lawhorn, N. Lu, J. Mao, H.B. Newman, J. Ngadiuba, T.Q. Nguyen, J. Pata, M. Spiropulu, J.R. Vlimant, C. Wang, S. Xie, Z. Zhang, R.Y. Zhu

California Institute of Technology, Pasadena, USA

J. Alison, M.B. Andrews, T. Ferguson, T. Mudholkar, M. Paulini, M. Sun, I. Vorobiev

Carnegie Mellon University, Pittsburgh, USA

J.P. Cumalat, W.T. Ford, E. MacDonald, T. Mulholland, R. Patel, A. Perloff, K. Stenson, K.A. Ulmer, S.R. Wagner

University of Colorado Boulder, Boulder, USA

J. Alexander, Y. Cheng, J. Chu, D.J. Cranshaw, A. Datta, A. Frankenthal, K. Mcdermott, J. Monroy, J.R. Patterson, D. Quach, A. Ryd, W. Sun, S.M. Tan, Z. Tao, J. Thom, P. Wittich, M. Zientek

Cornell University, Ithaca, USA

M. Albrow, M. Alyari, G. Apollinari, A. Apresyan, A. Apyan, S. Banerjee, L.A.T. Bauerdick, A. Beretvas, D. Berry, J. Berryhill, P.C. Bhat, K. Burkett, J.N. Butler, A. Canepa, G.B. Cerati, H.W.K. Cheung, F. Chlebana, M. Cremonesi, V.D. Elvira, J. Freeman, Z. Gecse, E. Gottschalk, L. Gray, D. Green, S. Grünendahl, O. Gutsche, R.M. Harris, S. Hasegawa, R. Heller, T.C. Herwig, J. Hirschauer, B. Jayatilaka, S. Jindariani, M. Johnson, U. Joshi, P. Klabbers, T. Klijnsma, B. Klima, M.J. Kortelainen, S. Lammel, D. Lincoln, R. Lipton, M. Liu, T. Liu, J. Lykken, K. Maeshima, D. Mason, P. McBride, P. Merkel, S. Mrenna, S. Nahn, V. O'Dell, V. Papadimitriou, K. Pedro, C. Pena⁵⁷, O. Prokofyev, F. Ravera, A. Reinsvold Hall, L. Ristori, B. Schneider, E. Sexton-Kennedy, N. Smith, A. Soha, W.J. Spalding, L. Spiegel, S. Stoynev, J. Strait, L. Taylor, S. Tkaczyk, N.V. Tran, L. Uplegger, E.W. Vaandering, H.A. Weber, A. Woodard

Fermi National Accelerator Laboratory, Batavia, USA

D. Acosta, P. Avery, D. Bourilkov, L. Cadamuro, V. Cherepanov, F. Errico, R.D. Field, D. Guerrero, B.M. Joshi, M. Kim, J. Konigsberg, A. Korytov, K.H. Lo, K. Matchev, N. Menendez, G. Mitselmakher, D. Rosenzweig, K. Shi, J. Sturdy, J. Wang, S. Wang, X. Zuo

University of Florida, Gainesville, USA

T. Adams, A. Askew, D. Diaz, R. Habibullah, S. Hagopian, V. Hagopian, K.F. Johnson, R. Khurana, T. Kolberg, G. Martinez, H. Prosper, C. Schiber, R. Yohay, J. Zhang

Florida State University, Tallahassee, USA

M.M. Baarmand, S. Butalla, T. Elkafrawy¹⁴, M. Hohlmann, D. Noonan, M. Rahmani, M. Saunders, F. Yumiceva

Florida Institute of Technology, Melbourne, USA

M.R. Adams, L. Apanasevich, H. Becerril Gonzalez, R. Cavanaugh, X. Chen, S. Dittmer, O. Evdokimov, C.E. Gerber, D.A. Hangal, D.J. Hofman, C. Mills, G. Oh, T. Roy, M.B. Tonjes, N. Varelas, J. Viinikainen, X. Wang, Z. Wu, Z. Ye

University of Illinois at Chicago (UIC), Chicago, USA

M. Alhousseini, K. Dilsiz⁹⁰, S. Durgut, R.P. Gandrajula, M. Haytmyradov, V. Khristenko, O.K. Köseyan, J.-P. Merlo, A. Mestvirishvili⁹¹, A. Moeller, J. Nachtman, H. Ogul⁹², Y. Onel, F. Ozok⁹³, A. Penzo, C. Snyder, E. Tiras, J. Wetzel

The University of Iowa, Iowa City, USA

O. Amram, B. Blumenfeld, L. Corcodilos, M. Eminizer, A.V. Gritsan, S. Kyriacou, P. Maksimovic, C. Mantilla, J. Roskes, M. Swartz, T.Á. Vámi

Johns Hopkins University, Baltimore, USA

C. Baldenegro Barrera, P. Baringer, A. Bean, A. Bylinkin, T. Isidori, S. Khalil, J. King, G. Krintiras, A. Kropivnitskaya, C. Lindsey, N. Minafra, M. Murray, C. Rogan, C. Royon, S. Sanders, E. Schmitz, J.D. Tapia Takaki, Q. Wang, J. Williams, G. Wilson

The University of Kansas, Lawrence, USA

S. Duric, A. Ivanov, K. Kaadze, D. Kim, Y. Maravin, T. Mitchell, A. Modak, A. Mohammadi

Kansas State University, Manhattan, USA

F. Rebassoo, D. Wright

Lawrence Livermore National Laboratory, Livermore, USA

E. Adams, A. Baden, O. Baron, A. Belloni, S.C. Eno, Y. Feng, N.J. Hadley, S. Jabeen, G.Y. Jeng, R.G. Kellogg, T. Koeth, A.C. Mignerey, S. Nabili, M. Seidel, A. Skuja, S.C. Tonwar, L. Wang, K. Wong

University of Maryland, College Park, USA

D. Abercrombie, B. Allen, R. Bi, S. Brandt, W. Busza, I.A. Cali, Y. Chen, M. D'Alfonso, G. Gomez Ceballos, M. Goncharov, P. Harris, D. Hsu, M. Hu, M. Klute, D. Kovalskyi, J. Krupa, Y.-J. Lee, P.D. Luckey, B. Maier, A.C. Marini, C. McGinn, C. Mironov, S. Narayanan, X. Niu, C. Paus, D. Rankin, C. Roland, G. Roland, Z. Shi, G.S.F. Stephans, K. Sumorok, K. Tatar, D. Velicanu, J. Wang, T.W. Wang, Z. Wang, B. Wyslouch

Massachusetts Institute of Technology, Cambridge, USA

R.M. Chatterjee, A. Evans, P. Hansen, J. Hiltbrand, Sh. Jain, M. Krohn, Y. Kubota, Z. Lesko, J. Mans, M. Revering, R. Rusack, R. Saradhy, N. Schroeder, N. Strobbe, M.A. Wadud

University of Minnesota, Minneapolis, USA

J.G. Acosta, S. Oliveros

University of Mississippi, Oxford, USA

K. Bloom, S. Chauhan, D.R. Claes, C. Fangmeier, L. Finco, F. Golf, J.R. González Fernández, C. Joo, I. Kravchenko, J.E. Siado, G.R. Snow[†], W. Tabb, F. Yan

University of Nebraska-Lincoln, Lincoln, USA

G. Agarwal, H. Bandyopadhyay, C. Harrington, L. Hay, I. Iashvili, A. Kharchilava, C. McLean, D. Nguyen, J. Pekkanen, S. Rappoccio, B. Roozbahani

State University of New York at Buffalo, Buffalo, USA

G. Alverson, E. Barberis, C. Freer, Y. Haddad, A. Hortiangtham, J. Li, G. Madigan, B. Marzocchi, D.M. Morse, V. Nguyen, T. Orimoto, A. Parker, L. Skinnari, A. Tishelman-Charny, T. Wamorkar, B. Wang, A. Wisecarver, D. Wood

Northeastern University, Boston, USA

S. Bhattacharya, J. Bueghly, Z. Chen, A. Gilbert, T. Gunter, K.A. Hahn, N. Odell, M.H. Schmitt, K. Sung, M. Velasco

Northwestern University, Evanston, USA

R. Bucci, N. Dev, R. Goldouzian, M. Hildreth, K. Hurtado Anampa, C. Jessop, D.J. Karmgard, K. Lannon, N. Loukas, N. Marinelli, I. Mcalister, F. Meng, K. Mohrman, Y. Musienko⁴⁹, R. Ruchti, P. Siddireddy, S. Taroni, M. Wayne, A. Wightman, M. Wolf, L. Zygala

University of Notre Dame, Notre Dame, USA

J. Alimena, B. Bylsma, B. Cardwell, L.S. Durkin, B. Francis, C. Hill, A. Lefeld, B.L. Winer, B.R. Yates

The Ohio State University, Columbus, USA

B. Bonham, P. Das, G. Dezoort, A. Dropulic, P. Elmer, B. Greenberg, N. Haubrich, S. Higginbotham, A. Kalogeropoulos, G. Kopp, S. Kwan, D. Lange, M.T. Lucchini, J. Luo, D. Marlow, K. Mei, I. Ojalvo, J. Olsen, C. Palmer, P. Piroué, D. Stickland, C. Tully

Princeton University, Princeton, USA

S. Malik, S. Norberg

University of Puerto Rico, Mayaguez, USA

V.E. Barnes, R. Chawla, S. Das, L. Gutay, M. Jones, A.W. Jung, G. Negro, N. Neumeister, C.C. Peng, S. Piperov, A. Purohit, H. Qiu, J.F. Schulte, M. Stojanovic¹⁸, N. Trevisani, F. Wang, A. Wildridge, R. Xiao, W. Xie

Purdue University, West Lafayette, USA

J. Dolen, N. Parashar

Purdue University Northwest, Hammond, USA

A. Baty, S. Dildick, K.M. Ecklund, S. Freed, F.J.M. Geurts, M. Kilpatrick, A. Kumar, W. Li, B.P. Padley, R. Redjimi, J. Roberts[†], J. Rorie, W. Shi, A.G. Stahl Leiton

Rice University, Houston, USA

A. Bodek, P. de Barbaro, R. Demina, J.L. Dulemba, C. Fallon, T. Ferbel, M. Galanti, A. Garcia-Bellido, O. Hindrichs, A. Khukhunaishvili, E. Ranken, R. Taus

University of Rochester, Rochester, USA

B. Chiarito, J.P. Chou, A. Gandrakota, Y. Gershtein, E. Halkiadakis, A. Hart, M. Heindl, E. Hughes, S. Kaplan, O. Karacheban²⁶, I. Laflotte, A. Lath, R. Montalvo, K. Nash, M. Osherson, S. Salur, S. Schnetzer, S. Somalwar, R. Stone, S.A. Thayil, S. Thomas, H. Wang

Rutgers, The State University of New Jersey, Piscataway, USA

H. Acharya, A.G. Delannoy, S. Spanier

University of Tennessee, Knoxville, USA

O. Bouhali⁹⁴, M. Dalchenko, A. Delgado, R. Eusebi, J. Gilmore, T. Huang, T. Kamon⁹⁵, H. Kim, S. Luo, S. Malhotra, R. Mueller, D. Overton, L. Perniè, D. Rathjens, A. Safonov

Texas A&M University, College Station, USA

N. Akchurin, J. Damgov, V. Hegde, S. Kunori, K. Lamichhane, S.W. Lee, T. Mengke, S. Muthumuni, T. Peltola, S. Undleeb, I. Volobouev, Z. Wang, A. Whitbeck

Texas Tech University, Lubbock, USA

E. Appelt, S. Greene, A. Gurrola, R. Janjam, W. Johns, C. Maguire, A. Melo, H. Ni, K. Padeken, F. Romeo, P. Sheldon, S. Tuo, J. Velkovska

Vanderbilt University, Nashville, USA

M.W. Arenton, B. Cox, G. Cummings, J. Hakala, R. Hirosky, M. Joyce, A. Ledovskoy, A. Li, C. Neu, B. Tannenwald, Y. Wang, E. Wolfe, F. Xia

University of Virginia, Charlottesville, USA

P.E. Karchin, N. Poudyal, P. Thapa

Wayne State University, Detroit, USA

K. Black, T. Bose, J. Buchanan, C. Caillol, S. Dasu, I. De Bruyn, P. Everaerts, C. Galloni, H. He, M. Herndon, A. Hervé, U. Hussain, A. Lanaro, A. Loeliger, R. Loveless, J. Madhusudanan Sreekala, A. Mallampalli, D. Pinna, A. Savin, V. Shang, V. Sharma, W.H. Smith, D. Teague, S. Trembath-reichert, W. Vetens

University of Wisconsin – Madison, Madison, WI, USA

† Deceased.

- ¹ Also at Vienna University of Technology, Vienna, Austria.
- ² Also at Institute of Basic and Applied Sciences, Faculty of Engineering, Arab Academy for Science, Technology and Maritime Transport, Alexandria, Egypt.
- ³ Also at Université Libre de Bruxelles, Bruxelles, Belgium.
- ⁴ Also at IRFU, CEA, Université Paris-Saclay, Gif-sur-Yvette, France.
- ⁵ Also at Universidade Estadual de Campinas, Campinas, Brazil.
- ⁶ Also at Federal University of Rio Grande do Sul, Porto Alegre, Brazil.
- ⁷ Also at UFMS, Nova Andradina, Brazil.
- ⁸ Also at Universidade Federal de Pelotas, Pelotas, Brazil.
- ⁹ Also at Nanjing Normal University Department of Physics, Nanjing, China.
- ¹⁰ Now at The University of Iowa, Iowa City, USA.
- ¹¹ Also at University of Chinese Academy of Sciences, Beijing, China.
- ¹² Also at Institute for Theoretical and Experimental Physics named by A.I. Alikhanov of NRC 'Kurchatov Institute', Moscow, Russia.
- ¹³ Also at Joint Institute for Nuclear Research, Dubna, Russia.
- ¹⁴ Also at Ain Shams University, Cairo, Egypt.
- ¹⁵ Also at Zewail City of Science and Technology, Zewail, Egypt.
- ¹⁶ Also at British University in Egypt, Cairo, Egypt.
- ¹⁷ Now at Fayoum University, El-Fayoum, Egypt.
- ¹⁸ Also at Purdue University, West Lafayette, USA.
- ¹⁹ Also at Université de Haute Alsace, Mulhouse, France.
- ²⁰ Also at Ilia State University, Tbilisi, Georgia.
- ²¹ Also at Erzincan Binali Yildirim University, Erzincan, Turkey.
- ²² Also at CERN, European Organization for Nuclear Research, Geneva, Switzerland.
- ²³ Also at RWTH Aachen University, III. Physikalisches Institut A, Aachen, Germany.
- ²⁴ Also at University of Hamburg, Hamburg, Germany.
- ²⁵ Also at Department of Physics, Isfahan University of Technology, Isfahan, Iran, Isfahan, Iran.
- ²⁶ Also at Brandenburg University of Technology, Cottbus, Germany.
- ²⁷ Also at Skobeltsyn Institute of Nuclear Physics, Lomonosov Moscow State University, Moscow, Russia.
- ²⁸ Also at Institute of Physics, University of Debrecen, Debrecen, Hungary, Debrecen, Hungary.
- ²⁹ Also at Physics Department, Faculty of Science, Assiut University, Assiut, Egypt.
- ³⁰ Also at MTA-ELTE Lendület CMS Particle and Nuclear Physics Group, Eötvös Loránd University, Budapest, Hungary, Budapest, Hungary.
- ³¹ Also at Institute of Nuclear Research ATOMKI, Debrecen, Hungary.
- ³² Also at Wigner Research Centre for Physics, Budapest, Hungary.
- ³³ Also at IIT Bhubaneswar, Bhubaneswar, India, Bhubaneswar, India.
- ³⁴ Also at Institute of Physics, Bhubaneswar, India.
- ³⁵ Also at G.H.G. Khalsa College, Punjab, India.
- ³⁶ Also at Shoolini University, Solan, India.
- ³⁷ Also at University of Hyderabad, Hyderabad, India.
- ³⁸ Also at University of Visva-Bharati, Santiniketan, India.
- ³⁹ Also at Indian Institute of Technology (IIT), Mumbai, India.
- ⁴⁰ Also at Deutsches Elektronen-Synchrotron, Hamburg, Germany.
- ⁴¹ Also at Sharif University of Technology, Tehran, Iran.
- ⁴² Also at Department of Physics, University of Science and Technology of Mazandaran, Behshahr, Iran.
- ⁴³ Now at INFN Sezione di Bari ^a, Università di Bari ^b, Politecnico di Bari ^c, Bari, Italy.
- ⁴⁴ Also at Italian National Agency for New Technologies, Energy and Sustainable Economic Development, Bologna, Italy.
- ⁴⁵ Also at Centro Siciliano di Fisica Nucleare e di Struttura Della Materia, Catania, Italy.
- ⁴⁶ Also at Università di Napoli 'Federico II', NAPOLI, Italy.
- ⁴⁷ Also at Riga Technical University, Riga, Latvia, Riga, Latvia.
- ⁴⁸ Also at Consejo Nacional de Ciencia y Tecnología, Mexico City, Mexico.
- ⁴⁹ Also at Institute for Nuclear Research, Moscow, Russia.
- ⁵⁰ Now at National Research Nuclear University 'Moscow Engineering Physics Institute' (MEPhI), Moscow, Russia.
- ⁵¹ Also at Institute of Nuclear Physics of the Uzbekistan Academy of Sciences, Tashkent, Uzbekistan.
- ⁵² Also at St. Petersburg State Polytechnical University, St. Petersburg, Russia.
- ⁵³ Also at University of Florida, Gainesville, USA.
- ⁵⁴ Also at Imperial College, London, United Kingdom.
- ⁵⁵ Also at P.N. Lebedev Physical Institute, Moscow, Russia.
- ⁵⁶ Also at Moscow Institute of Physics and Technology, Moscow, Russia, Moscow, Russia.
- ⁵⁷ Also at California Institute of Technology, Pasadena, USA.
- ⁵⁸ Also at Budker Institute of Nuclear Physics, Novosibirsk, Russia.
- ⁵⁹ Also at Faculty of Physics, University of Belgrade, Belgrade, Serbia.
- ⁶⁰ Also at Trincomalee Campus, Eastern University, Sri Lanka, Nilaveli, Sri Lanka.
- ⁶¹ Also at INFN Sezione di Pavia ^a, Università di Pavia ^b, Pavia, Italy, Pavia, Italy.
- ⁶² Also at National and Kapodistrian University of Athens, Athens, Greece.
- ⁶³ Also at Universität Zürich, Zurich, Switzerland.
- ⁶⁴ Also at Ecole Polytechnique Fédérale Lausanne, Lausanne, Switzerland.
- ⁶⁵ Also at Stefan Meyer Institute for Subatomic Physics, Vienna, Austria, Vienna, Austria.
- ⁶⁶ Also at Laboratoire d'Annecy-le-Vieux de Physique des Particules, IN2P3-CNRS, Annecy-le-Vieux, France.
- ⁶⁷ Also at Şırnak University, Sırnak, Turkey.
- ⁶⁸ Also at Department of Physics, Tsinghua University, Beijing, China, Beijing, China.
- ⁶⁹ Also at Near East University, Research Center of Experimental Health Science, Nicosia, Turkey.

- ⁷⁰ Also at Beykent University, Istanbul, Turkey, Istanbul, Turkey.
- ⁷¹ Also at Istanbul Aydin University, Application and Research Center for Advanced Studies (App. & Res. Cent. for Advanced Studies), Istanbul, Turkey.
- ⁷² Also at Mersin University, Mersin, Turkey.
- ⁷³ Also at Piri Reis University, Istanbul, Turkey.
- ⁷⁴ Also at Adiyaman University, Adiyaman, Turkey.
- ⁷⁵ Also at Ozyegin University, Istanbul, Turkey.
- ⁷⁶ Also at Izmir Institute of Technology, Izmir, Turkey.
- ⁷⁷ Also at Necmettin Erbakan University, Konya, Turkey.
- ⁷⁸ Also at Bozok Universitetesi Rektörlüğü, Yozgat, Turkey.
- ⁷⁹ Also at Marmara University, Istanbul, Turkey.
- ⁸⁰ Also at Milli Savunma University, Istanbul, Turkey.
- ⁸¹ Also at Kafkas University, Kars, Turkey.
- ⁸² Also at Istanbul Bilgi University, Istanbul, Turkey.
- ⁸³ Also at Hacettepe University, Ankara, Turkey.
- ⁸⁴ Also at Vrije Universiteit Brussel, Brussel, Belgium.
- ⁸⁵ Also at School of Physics and Astronomy, University of Southampton, Southampton, United Kingdom.
- ⁸⁶ Also at IPPP Durham University, Durham, United Kingdom.
- ⁸⁷ Also at Monash University, Faculty of Science, Clayton, Australia.
- ⁸⁸ Also at Bethel University, St. Paul, Minneapolis, USA, St. Paul, USA.
- ⁸⁹ Also at Karamanoğlu Mehmetbey University, Karaman, Turkey.
- ⁹⁰ Also at Bingol University, Bingol, Turkey.
- ⁹¹ Also at Georgian Technical University, Tbilisi, Georgia.
- ⁹² Also at Sinop University, Sinop, Turkey.
- ⁹³ Also at Mimar Sinan University, Istanbul, Istanbul, Turkey.
- ⁹⁴ Also at Texas A&M University at Qatar, Doha, Qatar.
- ⁹⁵ Also at Kyungpook National University, Daegu, Korea, Daegu, Republic of Korea.